Torsion of Rolled Steel Sections in Building Structures

JOHN G. HOTCHKISS

TORSIONAL STRESSES in a steel framed building are rarely serious enough to require design analysis. Many torsional situations can be disregarded completely. There are conceivable conditions, however, in which torsional loads can produce stresses of sufficient magnitude to require torsional analysis of a framing member.

It is important, therefore, that the structural engineer understand the principles of torsional behavior in rolled steel sections, and be able to recognize those special situations in which torsional loading may be significant to the design.

The purpose of this paper is to provide practical guidance to the designer in the evaluation and analysis of the effects of torsional loading on steel framing members. Design examples illustrate both a "short" approximate method of torsional analysis and a more exact method. A brief review of basic torsional theory and the torsional properties of rolled steel sections are included.

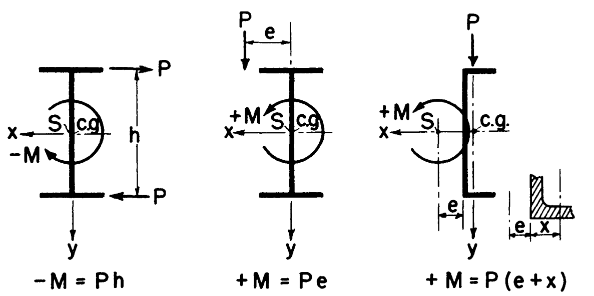

Figure 1

TORSIONAL BEHAVIOR

Torsional Loads —When a structural member is twisted about its longitudinal axis, it is said to be in torsion. Twisting is caused by external forces, moments or a couple acting on the member. Figure 1 shows these types of loads. The couple is composed of two parallel forces, equal in magnitude and opposite in direction. These forces are acting normal to the axis of the member. The usual torsional loading is that of a vertical load P, which does not pass through the shear center S, of the cross-section. The distance from load P to the shear center S is called the eccentricity, e. The eccentric moment that induces torsion on the cross-section is Pe. This moment is called M. (In this paper M represents a concentrated torsional moment, and m represents a uniformly distributed torsional moment induced in a member.)

John G. Hotchkiss is Senior Regional Engineer, American Institute of Steel Construction, New York, N. Y.

Effects of Induced Torsion—The aforementioned types of torsional loading are the cause of twisting in a member. The effect of this twisting can be threefold in a WF, I and [-section: torsional shear stresses, torsional warping shear stresses and torsional normal (longitudinal bending) stresses. These additive stresses often occur together with shear and normal stresses due to plane bending. Of these torsional effects, the magnitude of the torsional normal stresses is much greater than any of the other torsional stresses. The emphasis on normal stresses resulting from torsion will be discussed later in this paper.

Internal Equilibrium—The development of torsional stresses in a cross-section of a member is the result of internal resisting moments, which balance the applied moment M or m. For torsional equilibrium, then, the fundamental equation is

$$M_t = M_p + M_s \tag{1}$$

where M_t is the total of the internal resisting moments producing torsional shear, M_p is a torsional resisting moment called *primary torsion* (M_p is also known as "St. Venant's" torsion, "pure" torsion and "unrestrained" torsion), M_s is a *secondary* torsional moment which expresses warping resistance of a cross-section (M_s is often called "warping" torsion). Actually, Equation (1) is a statement of shear equilibrium, as both M_p and M_s produce shearing stresses. It is generally assumed that normal stresses σ, resulting from primary torsion M_p are negligible, unless the angle of twist is very large.

Analogy between Torsion and Plane Bending—Figure 2 shows a wide flange beam loaded at midspan with a concentrated torsional load M equal to unity. As shown, the ends of the beam are considered simply framed, AISC Type 2 construction, where it is assumed that the ends of the beam are free to rotate under loading which produces *plane bending*. A web connection consisting of two clip angles may be considered as Type 2 construction (See Fig. 8b). Under *torsional loading*, however, this connection prevents twisting of the beam about its longitudinal axis at the connection, since the web is restrained.

At any cross-section of the beam from **A** to **C** the internal moment M_t equals M_1, and from **C** to **B**, M_t equals $-M_2$. It can be seen also that $M_1a - M_2b = 0$ and $M_1 + M_2 = M$, and finally the following expressions

$$M_1 = \frac{b}{l} M \text{ and } M_2 = \frac{a}{l} M \tag{2}$$

An interesting analogous relationship is suggested by Equation (2). The analogy exists between the shear diagram due to plane bending and the moment diagram due to torsional twisting (Fig. 2). If a concentrated load P is applied at midspan, the shear at each end of the beam will be $V = P/2$. In the case of a torsional concentrated load M at midspan, the end moments M_1 and M_2 are equal to M_t, and $M_t = M/2$.

The moments M_1 and M_2 are determined in the same manner as the reactions at **A** and **B** due to a single load at **C**. It should be emphasized explicitly that this simple, apparently obvious analogy is by no means valid in general. For beams framed with Type 2 construction, the assumption that $M_t = M_1$ and M_2 at ends **A** and **B** is valid and Equation (2) is directly analogous. However, when beams are framed with Type 1 connections (welded, fully rigid) this assumption is not always strictly valid because of unsymmetrical loading conditions and the redundancy of the supports. Table 1 makes this distinction, and exact values are given when this analogy is not strictly valid. For beams subjected to a uniform torsional loading m, the same comments and restrictions for concentrated torsional loads apply.

Influence of M_p—The torsional resisting moment M_p is well named "primary", because it always appears to some extent in a beam under torsion. It is zero in a cross-section only when that cross-section is completely restrained against warping, such as at a fully welded connection. (See Case 5, Table 1.) In Fig. 3b, the cross-section at midspan must remain planar due to symmetry of load M (note that the angle of twist $\phi = 0$ at each end, viz., no twisting). Thus, since this cross-section at midspan is completely restrained against warping, $M_p = 0$ also. Warping is defined as a plane which when acted upon by forces, no longer remains planar; it warps out of plane.

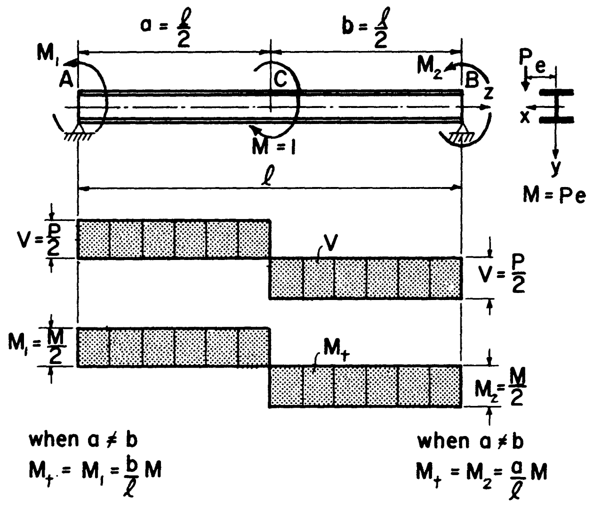

Figure 2

The fundamental equation for primary torsion, for *non-circular* sections, is

$$M_p = GK\phi' \tag{3}$$

where G is the shear modulus, ϕ' is the first derivative of ϕ (the angle of twist) with respect to z, and K is a torsional constant which describes the *torsional resistance* of a cross-section, and is based upon the geometry of the profile. Values for the torsional constant K for rolled steel sections have been published by Bethlehem Steel Corp.[1] Reference should also be directed to a recent paper by El Darwish and Johnston[6] covering an accurate calculation of this constant. For cross-sections made-up of *welded plates*, values for K can be computed from Chart 1.

Equation (3) shows that M_p is directly proportional to G, K, and ϕ', whereas ϕ' is indirectly proportional to GK, where GK is the *torsional rigidity* of the cross-section. Thus as K is increased, M_p increases. This means that M_p will offer a greater resistance to twisting action. The larger values for K appear for the larger (thicker) beam sections. For example, $K = 68.80$ for a 36 WF 300 section, whereas, $K = 0.195$ for a 5WF16 section.[1]

The influence of M_p is shown in Figs. 3a and 3b. In Fig. 3a, a solid circular cross-section is loaded at midspan with a torsional moment $M = 1$. At the ends, $M_p = M_t = M/2$ and $\phi = 0$. Since a circular section cannot warp (warpfree), M_p is constant for each half of the beam. From Equation (1), $M_t = M_p + 0$, where $M_s = 0$ and there is no warping. For circular sections, then, $M_p = M_t$, and M_p is exactly analogous to the shear diagram in plane bending. In Fig. 3b a WF section is loaded at midspan with a torsional moment $M = 1$. The noticeable difference between Fig. 3a and Fig. 3b is the curve for M_p. Since WF, I and [-sections are free

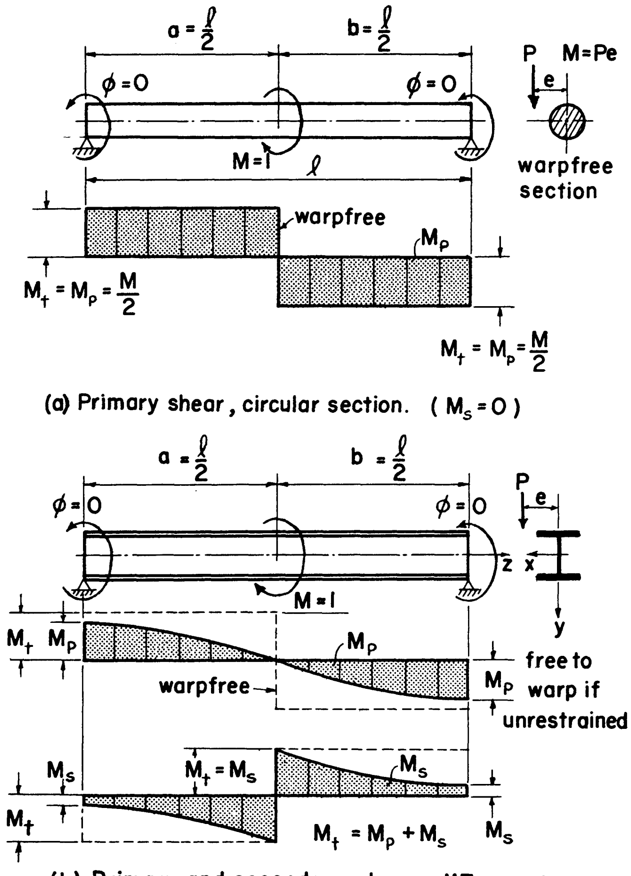

(a) Primary shear, circular section. ($M_s = 0$)

(b) Primary and secondary shear, WF- section

Figure 3

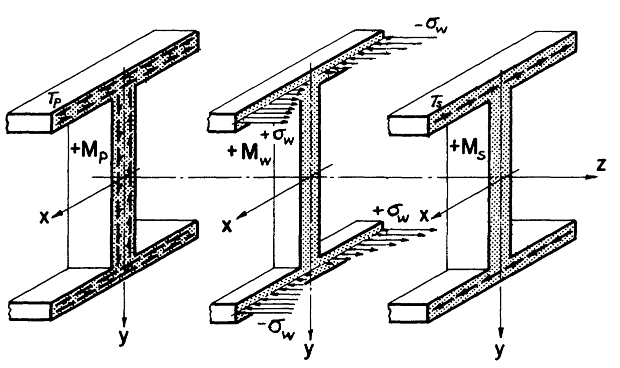

Torsional stresses

Figure 4

to warp if unrestrained, M_p no longer equals M_t. An increment of M_t is made up by the contribution of M_s as warping torsion. At midspan, where due to symmetry the cross-section remains planar, $M_p = 0$ as in Fig. 3a.

Influence of M_s—Figure 3b also shows the influence of M_s. At midspan where the cross-section is prevented from warping, the warping resistance is maximum. Here $M_s = M_t = M/2$. Since the sum of M_p and M_s equals M_t, the curves for M_p and M_s are complementary.

As M_s expresses warping resistance, a distinction must be made between various profiles as to their warping characteristics. One way is to refer to a *warping resistance constant*, known as C_w. Approximately exact values for C_w are tabulated in Table 4 for all rolled sections commonly used. Other values for C_w can be computed for sections of built-up welded plates by using the equations in Chart 1 and 2. For rolled WF sections

$$C_w = \frac{I_y}{2}\frac{h^2}{2} \text{ or } \frac{I_y h^2}{4} \qquad (4)$$

Chart 1 shows the equations for C_w for several built-up cross-sections. For rolled sections, C_w is negligible for T and L-sections. WF, I and [-sections, on the other hand, are free to warp if unrestrained and warping effects must be considered. Sections made up of not more than *two* rectangular elements do not warp, because of the fact that the middle planes of each element pass through the shear center. For WF, I and [-sections, the middle planes of *every* element do not pass through the shear center (Chart 2).

The warping resistance for moment M_s is determined from the equation

$$M_s = -EC_w\phi''' \qquad (5)$$

where E is the modulus of elasticity and ϕ''' is the third derivative of ϕ. From this equation it is seen that the warping resistance constant C_w is directly proportional to the moment M_s and indirectly proportional to the angle of twist ϕ. When $C_w = 0$ as in circular sections, $M_s = 0$, as was shown in Fig. 3a. In Equation (5) the term EC_w is actually a measure of the *warping rigidity* of a cross-section. In Equation (3) the term GK is a measure of the *torsional rigidity* of a cross-section. Both of these terms, influenced by the geometry of the cross-section, are important to torsional behavior. The ratio of these rigidities appears in another torsional constant called λ, which is tabulated for all rolled sections in Table 4. λ is a constant that describes the rate of decrease of the warping stresses and is found from

$$\lambda = \sqrt{\frac{GK}{EC_w}} \text{ (in.}^{-1}\text{)} \qquad (6)$$

Torsional Stresses Resulting from M_p **and** M_s—The result of torsional moments M_p and M_s in a member is shearing stress. Figure 4 shows the cross-section of a WF profile under the influence of M_p, M_w and M_s. The diagram for $+M_p$ shows that shearing stresses are developed in the flanges and web as a result of M_p. The diagram for $+M_s$ (warping) shows that the shearing stresses resulting from M_s appear only in the flanges. $+M_p$ and $+M_s$ follow sign convention when a positive

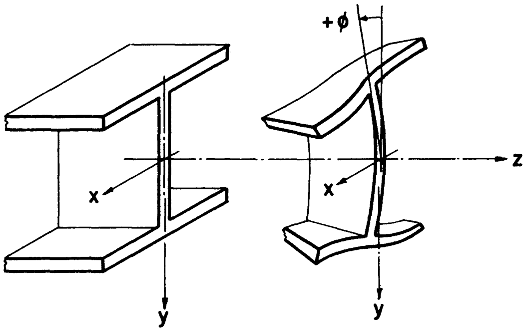

Positive angle of twist ϕ

Figure 5

angle of twist occurs as shown in Fig. 5. In terms of torsional shear magnitude, flange warping shear due to M_s is minor, compared to flange shear resulting from M_p; hence, M_s is called a secondary resisting moment.

The torsional shearing stress τ_p in the flanges or web of a WF, I or [-section due to M_p is determined from the equation

$$\tau_p = \frac{M_p t}{K} \tag{7}^*$$

where t is the thickness of flange or thickness of web.

Torsional shearing stresses in the flanges due to warping are found from

$$\tau_w = \frac{w_{\max} b}{4} \frac{M_s}{C_w} \tag{8}$$

where $w_{\max}$, shown in Chart 1, is the unit area of stress in the flange and b equals the width of the flange. For WF, I and [-sections $w_{\max} = w_a$. For [-sections w_a and w_b are required as shown in Chart 1. The values for w_a and w_b are tabulated in Table 4 for all rolled [-sections.

Torsional Normal Stresses Resulting from M_w—Thus far the discussion has been centered around two effects of twisting, namely M_p and M_s, and the associated shearing stresses. Of all the torsional effects in WF, I and [-sections, the additive effect of torsional normal stresses σ_w is the major consideration. The normal stresses σ_w are a result of torsional flange bending (induced by warping restraint) and are shown in Fig. 4. $+M_w$ is shown as the horizontal bending of the flanges producing normal stresses σ_w in the flanges. Torsional normal stresses σ_w must be added algebraically to the normal stresses σ_b produced by plane bending. Note in Fig. 4 the signs for stress σ_w follow the sign convention previously mentioned.

Normal stresses in plane bending are determined in the well-known manner by dividing the bending moment by a factor called section modulus. In torsional behavior, Prof. Bornscheuer[3, 4] suggests that the factor S_w be used as a warping modulus, and M_w as a moment (expressed as lb-in.^{2}),* to describe flange bending. This flange bending due to torsion is expressed by the equation

$$M_w = -EC_w\phi'' \tag{9}$$

Note that this equation is identical to Equation (5), except that the second derivative of ϕ is used here. The torsional normal stresses can be determined from

$$\sigma_w = \frac{M_w}{S_w} \tag{10}$$

In each of the Cases of Table 1, the two lower diagrams represent the curves for M_b and M_w. When plotted one above the other, the designer can quickly locate the ordinate to the curve which is maximum. Both the location and magnitude of the ordinate are given, and the additive effects of normal stresses can be quickly attained.

Summary of Torsional and Shears—In any WF, I or [-section under torsional loading, three internal moments occur, which are:

$M_p = GK\phi'$, which produces flange and web shear τ_p
$M_w = -EC_w\phi''$, which produces flange bending and flange normal stresses σ_w
$M_s = -EC_w\phi'''$, which produces warping shear τ_w in the flanges only.

From these equations it is seen that the only unknowns are the angle of twist ϕ and its three derivatives. In designing for torsion, ϕ is unknown; therefore, it has to be determined by the solution of the general differential equation.

However, the designer does not have to use this differential equation, since Table 1 has been set up for maximum torsional moments, which have been computed by determining the proper constants of integration and the location of maximum values. The simplified resulting equations are shown in each Case.

λl-Curves and Their Significance**—Figures 6a and 6b illustrate families of curves with varying parameters of λl. One family represents the M_p-curves

* *Generally accepted expression for shearing stress in flanges or web. Reference 6 has, for the first time, more accurately determined this expression. In some cases, particularly [-sections, Equation (7) may be low by 20 per cent for values of shear in the flanges.*

* *Bornscheuer uses the term "bimoment", since its dimension contains the second power of inches.*

** *Reference 7 provides more extensive curve-plots for all rolled sections.*

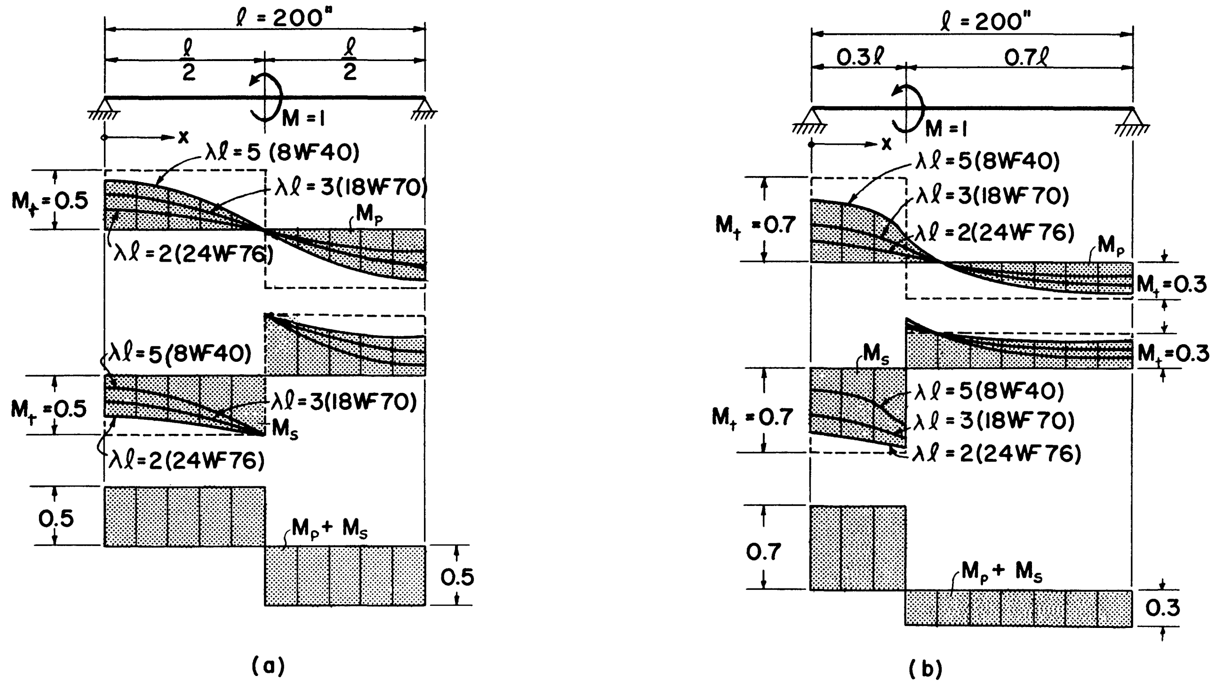

Figure 6

and the second family below it, the M_s-curves. The third diagram is the sum of the M_p- and M_s-curves and is a plot of Equation (1), $M_t = M_p + M_s$. As is true of any parameter, λl is fixed for each individual curve but differs from one curve to another in the same family.

Observation of Fig. 6a, with a unit torsional load at midspan, and Fig. 6b, with the same unit load at $x = 0.3l$, shows the complex nature of the curves involving hyperbolic functions. In Fig. 6a the family of M_p-curves ($\lambda l = 5$, 3 and 2) each have the same point of inflection at midspan. At each end of the beam where $x = 0$ and $x = l$, the ordinates at these points are maximum. As the parameter λl increases, the y-intercept to the M_p-curves becomes larger. Graphically, this indicates that the influence of M_p is greater, and has more resistance to twisting than M_s. Examination of the famliy of M_s-curves shows that the point of maximum ordinate occurs at midspan where the curves pass through the point of inflection. As λl increases, the y-intercept close to $x = 0.5l$ becomes smaller and the influence of λl is less noticeable.

By comparison, Fig. 6b shows the same family of curves, with different curvatures and a notable difference in the point of inflection for each λl-curve for values of M_p. The point of inflection not only is not under the load as would be expected, but has different x-intercepts. The point of maximum ordinate to the M_p-curve is at $x = 0$. In the case of the M_s-curves the point of inflection occurs under the load at $x = 0.3l$. The maximum ordinates to the curve are at the point of inflection. The higher values of λl yield smaller y-intercepts and M_s contributes less in resisting the twisting of the beam.

The three curves of each diagram represent $\lambda l = 2$, $\lambda l = 3$ and $\lambda l = 5$. In order that their significance be meaningful in a practical sense, three beams have been selected from Table 4 whose λ values, when multiplied by the span length l, correspond to the λl values plotted. The span length l is arbitrarily taken as 200 in. The beam sections and their λ values are as follows: 24 WF 76, $\lambda = 0.0103$; 18 WF 70, $\lambda = 0.01475$; 8 WF 40, $\lambda = 0.0245$.

Chart 3 gives the computed values for the ordinates to the M_p-, M_s- and M_t-curves in Fig. 6. It can be seen that the sum of the M_p and M_s ordinates all add to the sum of 0.50, which agrees with the diagram for M_t in Fig. 6a. The analogy between the shear diagram and the M_t diagram is strictly valid for this case of loading and end support. Therefore, $M_t = 0.5M$.

Figure 7 illustrates the family of M_w-curves located under the moment diagram for unit load at $x = 0.3l$ producing plane bending. The parameters plotted are $\lambda l = 5$, 3 and 2 as used in Fig. 6a and Fig. 6b. The maximum ordinate to the M_w-curve appears at $x = 0.3l$ where each curve has a marked cusp. The maximum ordinate to the M_w-curve for symmetrical torsional loading also occurs under the point of loading and will correspond to the same location for the maximum ordinate to the M_p-curve.

As the λl values increase, the y-intercept becomes greater. It can be seen from this figure that a greater warping resistance is required of a cross-section as λl increases. When heavier, thicker beam sections are selected, the ordinate to the M_w-curve becomes smaller, indicating that the geometry of the section has less tendency to warp and consequently the normal stresses developed will be of a lower magnitude.

The various Cases shown in Table 1 include only one curve for the parameter λl. It was not necessary to plot other λl-curves, since in practice the designer is primarily concerned with the location and magnitude of maximum ordinates to the curves. Equations to the right of the diagrams provide this information. After studying the curves in Fig. 6a and Fig. 6b it will be evident that one curve of a family exhibits certain common characteristics compared to other curves in the family. All curves of the same family have the same concavity viz., concave upwards or concave downwards. All curves at any y-intercept have the same sign for curve slope $m = \Delta y/\Delta x$ viz., Δy increases or Δy decreases, indicating negative and positive slope respectively. Graphically this tells the designer the important condition as to whether the function under study is increasing or decreasing at any point along the beam span.

END RESTRAINTS

The condition of an end restraint is important in torsional analysis, as it is in plane bending. In building construction, and for *plane bending*, the AISC suggests three types of end restraint, namely: Type 1—fully-fixed beams, Type 2—simple connections, and Type 3—semi-rigid framing (partially restrained). In torsional analysis, only Types 1 and 2 will be considered (Fig. 8).

A Type 1 connection, in which the beam-end is fully welded around the flanges and web, offers only partial warping restraint and $M_p \neq 0$, as is found in many references. This restraint may range from 20 to 60 percent. In order to assume $M_p = 0$ as shown in Fig. 8 and the diagrams in Table 1, the ends of the beam must be boxed-in. This can be simply taken care of by welding stiffener plates between the toes of the flanges. To be effective in the end zone of the beam, the length of these stiffeners along the longitudinal axis of the beam must be equal to or greater than the depth d of the beam. The designer should also take into consideration the torsional characteristics of the column in a beam-to-column connection. Where the rigid box-ended beam connects to a column with torsionally soft flanges it is advisable to provide column stiffeners between the flanges at the point of load application (see Design Example 1). In Type 2, which is considered as a typical web connection made up of two clip angles, the twisting at the connection is prevented and $\phi = 0$. However, it should be recognized that the L distance of the clip

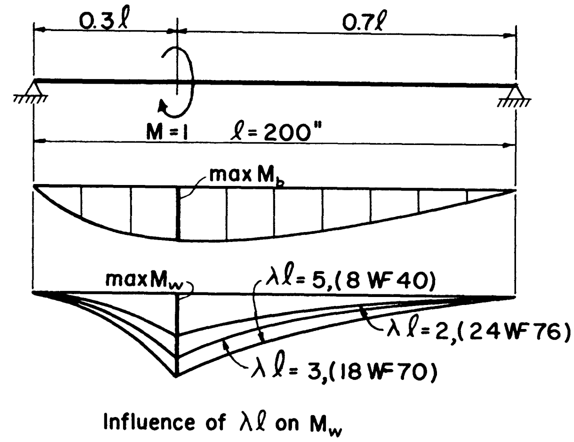

Figure 7

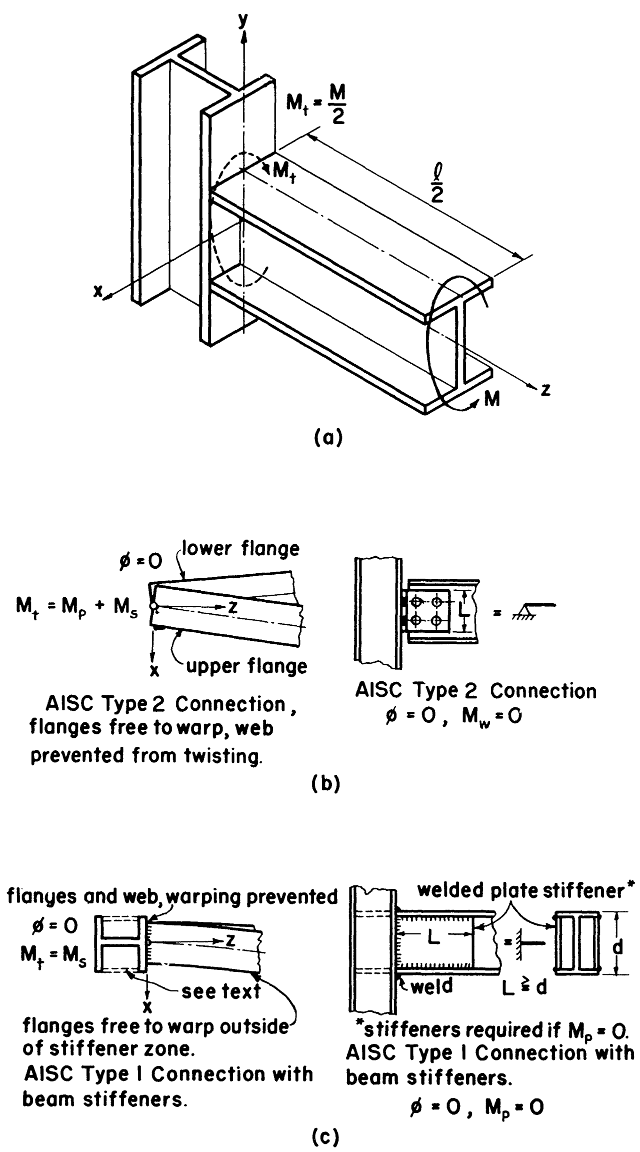

Figure 8

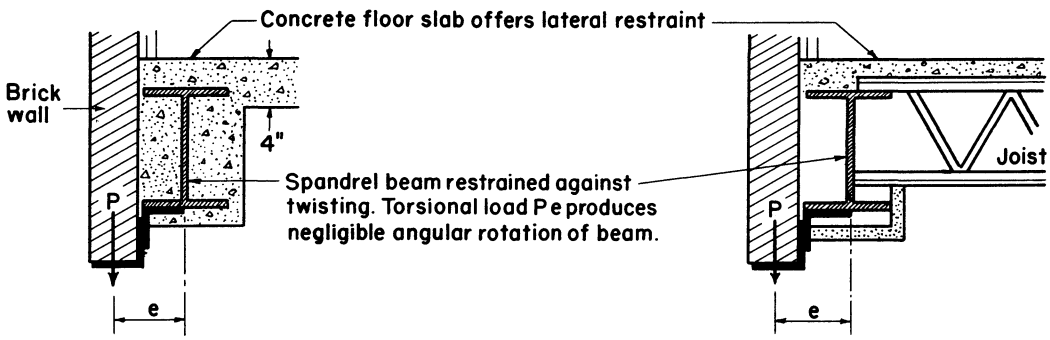

Fig. 9. Uniform torsional loading with no torsional stress effect

angles must extend over the major depth of the web in order that the assumption $\phi = 0$ is reasonably valid.

What are the effects of end restraint on M_p, M_w and M_s? Figures 8b and 8c show Type 1 and 2 connections, where for Type 1, $\phi = 0$ and $M_p = 0$; for Type 2, $\phi = 0$ and $M_w = 0$.

For torsional equilibrium, $M_t = M_s$ as shown in Fig. 8c. In the Type 2 connection the beam does not twist at the connection. However, since the flanges can displace as shown in Fig. 8b, there is no restraint to flange bending and $M_w = 0$. The equilibrium of torsional moments is $M_t = M_p + M_s$. Actually, M_s would be zero at the ends if the beam were twisted by an equal and opposite moment at each end. This condition of pure torsion will rarely be found in structural practice.

PRACTICAL DESIGN CONSIDERATIONS

The occasions in actual practice where torsional problems arise are few in number, when considering building design. When such occasions occur, however, certain preliminary questions should be proposed. Will the torsional load produce significant twisting? Are there any restraining effects which will prevent twisting?

When an appreciable torsional moment is known to exist, the most satisfactory solution is to use a full length welded box girder. Usually with appreciable torsion, the box girder will take no more material than a heavy rolled section with welded end stiffeners.

In building design, most structural members are laterally restrained because of attachments to the structure along the length of the member. Rarely will the designer find a beam that is totally unrestrained viz., free to twist over its entire length. Hence, a good many cases involving torsional loading show that lateral restraints, existing in the form of attachments to the member, prevent twisting and torsional stresses can be ignored. This condition may be considered as torsion that is self-limiting. It is of no consequence when limited by the permissible end slope of the attaching members.

Based upon this evidence, beams that are a part of the floor assembly in buildings are usually restrained by a floor slab and, therefore, the torsion is simply self-limiting. Figure 9 illustrates this point where a typical spandrel beam is under a one-sided loading. The torsional load does not pass through the shear center. Normally, this loading would introduce torsional moments and subsequent torsional shearing and bending in the beam. In Fig. 9a the floor assembly consists of a concrete floor slab, usually not less than 4 in. in thickness, spanning not over 8 ft between intermediate beams. In order that the spandrel beam can twist under this eccentric loading, the entire floor assembly would have to rotate as well. Although the concrete slab in Fig. 9b is only 2½ in. thick, it also offers continuous and adequate lateral support against torsional twisting. Since twisting is prevented, it is safe to assume that normal stresses due to torsion can be ignored and no torsional analysis will be required.

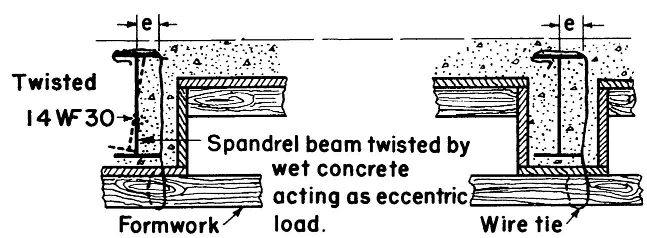

Fig. 10. Uniform torsional loading produces torsional stresses

Beam Twists During Erection—When significant twisting occurs in building construction, it will probably be during erection, before all the final loads are applied. During the erection of building structures, while temporarily unbraced, an unbalanced loading condition may produce excessive twisting. A few years ago, the writer investigated steel beams twisted by torsional loading as a result of improper field practice. The case involved spandrel and header beams in a school building, which were twisted as much as 17 degrees. The twisting was due to unbalanced loading as shown in Fig. 10.

The formwork for the concrete slab was supported by wire ties wrapped around the top flange of the beams. All wire supports, however, were carried down on one side of the beam only. These wire ties supported the entire weight of the wet concrete. The one-sided support introduced an eccentricity equal to one-half of the flange width.

Since the beams were sized for plane bending only, they were torsionally weak. Had the wire ties been carried down on alternate sides of the beam, the unbalanced loading condition would never have occurred.

Improving the Torsional Rigidity—One means of improving the torsional rigidity of a rolled steel section is by the addition of new material, thus altering the K-value of the section—restricted, however, to that zone where the additional material occurs (Fig. 12). In other zones of the beam the effect is indirect. As an example, when a plate is welded between each flange at the toes, as in Fig. 11, the K-factor is increased considerably. In this instance K is increased to 3,246, approximately one hundred times the original value. The addition of these plates is analogous to the addition of cover plates to a beam under plane bending. It should be pointed out that the addition of these plates prevents the flanges from deforming; consequently warping effects become nil. The resulting closed box section is treated as being under primary shear only.

In passing, the engineer will recognize another familiar case of torsion and unsymmetrical bending resulting from biaxial bending, where a torsionally weak rolled section has to be reinforced. This is in the design of crane runway girders. It is common practice to assume that the bending moment caused by the horizontal loading is resisted by the upper flange. Accordingly, the top flange is reinforced.

GENERAL REMARKS

If torsional loading is known to produce significant twisting, and analysis of the torsional plus direct bending stresses shows the stresses are too high, the following solutions may be employed: (1) furnish a full length box girder section instead of a rolled section, (2) provide additional lateral supports, or braces, which will torsionally restrain the twist, (3) select a rolled section whose value of λ is of a lower value than the one which is highly stressed, and (4) consider the addition of welded plates between the flanges as just described (see Fig. 12). The improved torsional rigidity of steel beams encased in concrete for fire protection requirements should not be overlooked.

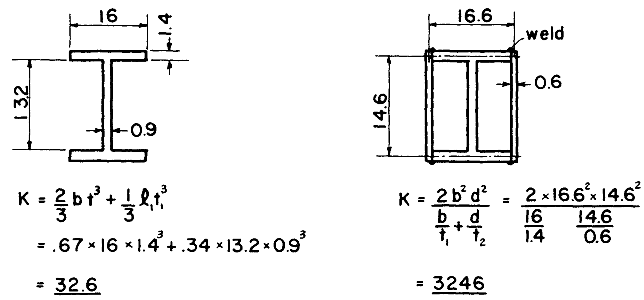

Fig. 11. Effect of stiffeners

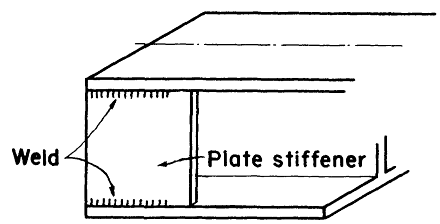

Fig. 12. Use of end stiffeners

DESIGN EXAMPLES

As stated previously, three types of torsional stresses are produced as a result of torsional loading on thin-walled open profiles such as a WF, I or [-section: (1) normal (bending) stresses in the flanges, critical at the toes, (2) primary shear stresses in the flanges and web, critical at the juncture of the web and flange, and (3) secondary warping shear stresses in the flanges, not critical and normally disregarded in stress analysis.

Of major concern in torsional analysis is the increase in bending stresses at the toes of the flanges which must be added to the direct bending stresses. Therefore, in any torsional design the first step is to determine the location of the maximum torsional moment M_w, and then determine the maximum normal stresses. Reference to Table 1 for the type of loading and nature of end restraint will give the location of the maximum ordinate to the M_w-curve. With a few minor exceptions, this location, as appearing in the diagrams, is applicable to all λl-curves of the same family. Where this is not true, an $\bar{x}$-distance is given for several λl-values. A linear interpolation can be made for intermediate values of λl.

The most frequently used loading condition is that of a concentrated torsional load M applied at some distance x from the left support, and a uniformly distributed load m applied over the entire span. For these conditions then, a "Short Method" is offered to the designer permitting him to evaluate the magnitude of

M_w and σ_w immediately before continuing an extensive torsional analysis. The results obtained by this method are then compared with the permissible stresses for combined bending and torsion. If the results are close to the allowable stresses established, then a more exact method should be undertaken. The design examples illustrate both methods.

Under the "Short Method", each of the two loading conditions just mentioned are treated separately for two cases of end restraint. Table 2 covers Type 2 construction (simple framing connection) and Type 1 construction (all welded, fully fixed connection) is covered by Table 3.

When a more exacting analysis is required, the designer may refer to Table 1 using the appropriate Case for loading and end restraint. Equations are given for computing the maximum M_w, M_p and M_s. For special conditions, an equation is given for M_w for any value of x along the span. With this information a complete λl-curve for M_w can be plotted. It will be found by the designer that under most circumstances the addition of torsional primary shear stresses is inconsequential.

Space does not permit the inclusion of the derivation of the general differential equation, nor the complete solution of this equation for numerous other conditions of loading and end support (see References 3, 13, 15).

Example 1

Given: An 18WF96 beam fixed at both ends is under a torsional load P, applied at the end of the bracket which is 71 in. long. (The eccentricity, e = 71 in. The torsional moment $M = 71 \times -400 = -28{,}400$ lb.-in.) (See Fig. 13.)

Solution:

From AISC Manual

I_x = 1674 in.^{4}
S_x = 184.4 in.^{3}
w = D. L. beam

From Table 4

w_{max} = 50.90 in.^{2}
I_w = 15,380 in.^{6}
S_w = 302.1 in.^{4}
λ = 0.01201 in.$^{-1}$

Normal stresses:

$$\sigma_b = \frac{M_b}{S}, \sigma_s = \frac{M_w}{S_w}$$

where

M_b = plane bending and M_w = flange bending (torsion)

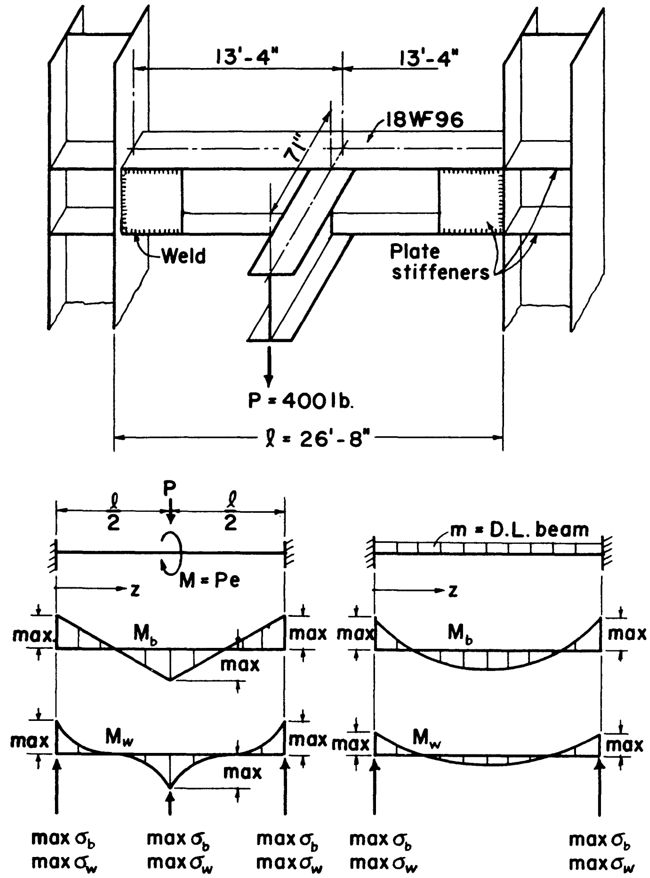

See TABLE I Case 10 & 5 and Short Method in TABLE 3.

Figure 13

1. From moment curves in diagram it is seen that the controlling condition will be when moments are combined at the end supports, for the determination of normal stresses.
2. Determine the moments and normal stresses due to plane bending:

Load P:

$$M_b = \frac{Pl}{8} = \frac{400 \times 320 \text{ in.}}{8} = -16{,}000 \text{ lb.-in.}$$

(max at center and ends)

$$\sigma_b = \frac{M}{S} = \frac{16{,}000}{184.4} = 86.7 \text{ psi}$$

Load w:

$$M_b = \frac{wl^2}{12} = \frac{96 \times (26.66)^2}{12} = -5{,}700 \text{ lb.-ft.}$$

(max at ends)

$$\sigma_b = \frac{M}{S} = \frac{5{,}700 \times 12}{184.4} = 371 \text{ psi}$$

3. Determine the moments and normal stresses due to warping torsion:

   Quick Method: Use of influence lines in Table 3.

   The following values are required:

   Let $\gamma = \lambda l = 0.01201 \times 320 = 3.84$, $\eta = 0.370$, where η is found by entering Table 3 with $z/l = 160/320 = 0.5$, proceed to curve where $\gamma = 3.84$. The desired value of η at the left is 0.370.

   The moment M_w, due to flange bending, for $z = 0$ is

$$M_w = \frac{1}{\lambda}\,\eta M = \frac{1}{0.01201}\,0.370 \times (-28{,}400) = -876{,}000 \text{ lb.-in.}^2$$

   The normal bending stress is

$$\sigma_s = \frac{M_w}{S_w} = \frac{876{,}000}{302.1} = 2{,}900 \text{ psi}$$

   The normal stresses are as shown in Fig. 14.

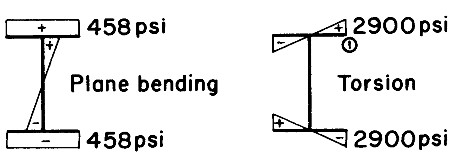

Figure 14

At point ①, $\max \sigma = \max \sigma_b + \max \sigma_s = 458 + 2{,}900 = 3{,}358$ psi

Conclusion: Since σ_{max}, due to combined bending and torsion, is well below any allowable stress limit it is unnecessary to proceed to a more extensive analysis.

Example 2

Given: Assume the same conditions as Example 1 except for loading. Let m equal a uniformily distributed torsional load. Then $m = 100 \times 7 = 700$ lb.-in./ft or 58.4 lb.-in./in. (See Fig. 15.)

Solution:

Quick Method

1. Determine warping moment M_w from influence lines Table 3.

   Let $\gamma = \lambda l = 0.01201 \times 320 = 3.84$ and $1/\lambda^2 = 6{,}940$

   Enter tabular values at right with $\gamma = 3.84$ and find area $A \cong -1.07462$.

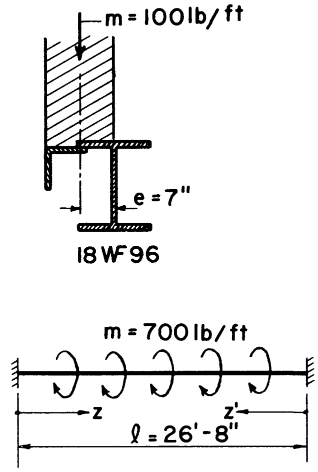

Figure 15

Warping moment M_w for $z=0$ equals $1/\lambda^2 Am$ where $m = 58.4$ lb.-in./in.

$$M_w = 6940 \times (-1.0746) \times 58.4 = -436{,}000 \text{ lb.-in.}$$

$$\max \sigma = \frac{-436{,}000}{302.1} = -1{,}450 \text{ psi}$$

This stress would then be added to any bending stresses resulting from plane bending.

Exact Method

Table I, Case 5

Warping moment $M_w = -EC_w\phi''$

$$= \frac{m}{\lambda_2}\left(1 - (1-k)\frac{\sinh \lambda z + \sinh \lambda z'}{\sinh \lambda l}\right)$$

where

$$\lambda l = 3.84$$

$$\lambda z = 0.01201 \times 0 = 0$$

$$\lambda z' = \lambda l$$

$$k = 1 - \frac{\lambda(l/2)}{\tanh \lambda(l/2)} = 1 - \frac{1.92}{0.95792} \doteq -1$$

$$M_w = 58.4\,(6{,}940)\left(1 - (1+1)\,\frac{0 + 22.5}{22.5}\right) = -406{,}000 \text{ lb.-in.}$$

$$\max \sigma = \frac{-406{,}000}{302.1} = -1{,}345 \text{ psi}$$

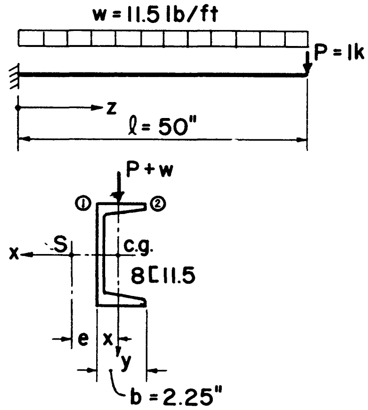

Figure 16

Example 3

Given: Cantilever beam loaded at its free end with a concentrated load $P = 1$ kip, acting through the c.g., point G. The dead load of beam will also be considered as acting through the c.g. (See Fig. 16.)

Solution:

From AISC Manual	*From Table 4*
$I_x = 32.3$ in.^{4}	$\lambda = 0.05873$ in.$^{-1}$
$S_x = 8.1$ in.^{3}	$S_w = 2.423$ in.^{4}
$x = 0.58$ in.	$I_w = 12.84$ in.^{5}
	$w_b = 2.555$ in.^{2}
	$w_a = -5.3$ in.^{2}
	$e = 0.5785$ in.

Loads: D.L. $w = 11.5$ lb./ft $= 0.96$ lb./in.
$P =$ 1 kip

Eccentricity: $= e + x = 0.5785 \times 0.58 = 1.16$ in.
Torsional moment due to D.L.:
$-0.96 \times 1.16 = -1.11$ lb.-in./in. $= -m$

Torsional moment due to P:
$-1000 \times 1.16 = -1{,}160$ lb.-in./in. $= -M$

The stresses at the fixed end are as follows:

Due to plane bending:

Bending moment due to w:

$$M_b = -\frac{0.96 \times 50^2}{2} = -1200 \text{ lb.-in.}$$

Bending moment due to P:

$$M_b = -1000 \times 50 = -50{,}000 \text{ lb.-in.}$$

Bending stresses due to w:

$$\sigma_b = \pm\frac{1{,}200}{8.1} = \pm 148 \text{ psi}$$

Bending stresses due to P:

$$\sigma_b = \pm\frac{50{,}000}{8.1} = \pm 6{,}170 \text{ psi}$$

Due to warping:

For warping calculations the following factors are needed:

$\lambda^2 = 0.05873^2 = 0.00345$
$\lambda l = 0.05873 \times 50 = 2.94$

From Table 2:

sinh $\lambda l = 9.431$
cosh $\lambda l = 9.484$
tanh $\lambda l = 0.9944$

Warping moment due to w:

From Case ⑥ where $z = 0$ and $\lambda l \sinh \lambda z = 0$:

$$M_w = \frac{m}{\lambda^2}\left[1 + 0 - \frac{(1 + \lambda l \sinh \lambda l) \times 1}{\cosh \lambda l}\right]$$

$$= \frac{-1.11}{0.00345}\left[1 - \frac{(1 + 2.94 \times 9.431)}{9.484}\right]$$

$$= +654 \text{ lb.-in.}^2$$

Warping moment due to P:

From Case ⑦ where $z' = l$ and $\frac{\sinh}{\cosh} = \tanh$:

$$M_w = \frac{M}{\lambda}\left(-\frac{\sinh \lambda l}{\cosh \lambda l}\right)$$

$$= \frac{-1.11}{0.05837} \times (-0.9944) + 19{,}720 \text{ lb-in.}^2$$

Warping stresses due to w at points ① and ②:

$$\sigma_2 = \frac{M_w}{S_w} \frac{+654}{-2.423} = -270 \text{ psi}$$

$$\sigma_1 = \frac{M_w}{I_w} \times w_1 \frac{+654}{12.84} \times 2.555 = +130 \text{ psi}$$

Warping stresses due to P:

$$\sigma_2 = \frac{+19720}{-2.423} = -8{,}140 \text{ psi}$$

$$\sigma_1 = \frac{+19720}{12.84} \times 2.555 = +3{,}920 \text{ psi}$$

The total longitudinal bending stresses in the upper flange at points ① and ② are:

Pt. ①: $\sigma = +148 + 6{,}170 + 130 + 3{,}920 = +10{,}368$ psi

Pt. ②: $\sigma = +148 + 6{,}170 - 270 - 8{,}140 = -2{,}092$ psi

The largest combination appears at Pt. ①.

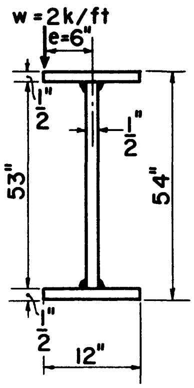

Figure 17

Example 4

Given: A beam built-up by welding three plates resembling an I-section is loaded with a uniformily distributed torsional moment $m = 1000$ lb.-ft/ft over the entire span of 46 ft. The end connections are assumed to be bolted web clip angles, Type 2 construction. Determine if the additive torsional normal stresses are within permissible limits by the "Quick Method". ($e = 6$ in., $w = 2{,}000$ lb./ft.) (See Fig. 17.)

Solution:

$m = w_e = 2{,}000 \times 0.5 = 1{,}000$ lb.-ft/ft (positive moment, see Fig. 5)

Determine the torsional constants and properties from Chart 1:

$$C_w = \frac{1}{24} b^3h^2t = \frac{1}{24} 12^3 \times 53.5^2 \times 0.50$$

$$= 103{,}000 \text{ in.}^6$$

$$K = \frac{2}{3} bt^3 + \frac{1}{3} l_1t_1^3$$

$$= \frac{2}{3} \times 12 \times 0.50^3 + \frac{1}{3} \times 53 \times 0.50^3$$

$$= 3.21 \text{ in.}^4$$

$$w_{\max} = \frac{bh}{4} = \frac{12 \times 53.5}{4} = 160.5 \text{ in.}^2$$

$$\lambda = 0.62\sqrt{\frac{K}{C_w}} = 0.62\sqrt{\frac{3.21}{103{,}000}} = 0.00341 \text{ in.}^{-1}$$

$$\lambda l = 0.00341 \times 552 = 1.88$$

$$S_w = \frac{C_w}{w_{\max}} = \frac{103{,}000}{160.5} = 642 \text{ in.}^4$$

Determine max. warping bimoment M_w at midspan by using Table 2, Quick Method. Since $\lambda l = 1.88$, a linear interpolation between $\lambda l = 1.5$ and 2.0 gives 0.0893. Then max. $M_w = 0.0893\, ml^2 = 0.0893 \times 1{,}000 \times 46^2 = 189{,}000$ lb.-ft.

$$\max \sigma_w = \frac{M_w}{S_w} = \frac{189{,}000}{642} = 3{,}540 \text{ psi}$$

Determine max. moment due to plane bending at midspan:

$$\max M_b = \frac{wl^2}{8} = \frac{2{,}000 \times 46^2}{8} = 528{,}000 \text{ lb.-ft.}$$

$$\max \sigma_b = \frac{M_b}{S} = \frac{528{,}000}{547} = 11{,}600 \text{ psi}$$

Combined normal stresses: $\max \sigma_w + \max \sigma_b = 3{,}540 + 11{,}600 = 15{,}140$ psi (See Fig. 18.)

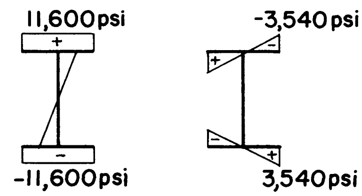

Figure 18

Check by long method using Table 1:

$$\max M_w = \frac{m}{\lambda^2}\left[1 - \frac{1}{\cosh \lambda l/2}\right]$$

where $\lambda l/2 = 0.94$ and $\cosh 0.94 = 1.475$

$$\max M_w = \frac{1000}{0.00341^2}\left[1 - \frac{1}{1.475}\right]$$

$$= 27{,}800{,}000 \text{ lb.-in.}$$

By quick method:
$27{,}800{,}000 \times 144 = 27{,}200{,}000$ lb.-in.

NOMENCLATURE

a Distance measured along the longitudinal axis of member (ft); distance from the shear center to the centerline of web in a channel (in.)

b Width of a flange (in.); length of a rectangular element (in.); distance measured along the longitudinal axis of a member (ft)

c Distance measured along the longitudinal axis of a member (ft)

d Depth of a section (in.)

e Eccentricity in a member; in a channel it is the distance from the shear center to the back of the channel web (in.)

f Subscript indicating flange; symbol for function

h Distance between centroids of flanges (in.)

l Span of a beam (ft)

l_1 Distance between flanges (in.)

m Uniformly distributed torsional load (lb.-ft/in.)

t Thickness of a flange (in.)

t_1 Thickness of a web (in.)

w_a, w_b Value of unit warping at points a and b of a flange for WF, I and [-sections, (in.^{2})

$w_{\max}$ Maximum value of unit warping, $w_{\max} = w_a$ for WF and I sections (in.^{2})

w_1, w_2 Value of unit warping at points 1 and 2 in the flanges of channel sections (in.^{2})

x Coordinate; the distance in a channel from the back of the web to the y-axis (in.)

y Coordinate; deflection in plane bending (in.)

z Coordinate

A Area of a section or rectangle (in.^{2}); area under influence line (in.^{2})

A_f Area of flange (in.^{2})

A_w Area of web (in.^{2})

C Constant of integration

C_w Warping resistance constant (in.^{6})

E Modulus of elasticity (psi)

G Shear modulus of elasticity (psi); center of gravity of a cross-section

I Moment of inertia (in.^{4})

K Torsional resistance constant; associated with St. Venant's torsion (in.^{4})

L Length of stiffener plate (in.)

M Applied concentrated torsional moment (lb.-ft)

M_b Moment due to plane bending (lb.-ft)

M_p Primary or pure torsional resisting moment (lb.-ft) associated with St. Venant's torsion

M_s Secondary warping torsional resisting moment (lb.-ft); associated with warping torsion

M_t Total torsional resisting moment at any given cross-section, where $M_t = M_p + M_s$ (lb.-ft)

M_w Warping coefficient of loading and support condition; associated with warping forces and used to determine flange bending (lb.-in.^{2})

P Concentrated load (lb.)

S Shear center of a cross-section

S_w Warping section modulus (in.^{4})

$S_{x,y}$ Section modulus about x or y axis (in.^{3})

γ Parameter where $\gamma = \lambda l$ (dimensionless)

θ Unit angle of twist (radians/in.)

λ Torsional constant, $\lambda = \sqrt{GK/EC_w}$ (in.$^{-1}$)

ρ Radius of curvature (in.)

σ Normal unit bending stress (psi)

σ_b Normal stress associated with plane bending (psi)

σ_p Normal stress associated with primary torsion (psi)

σ_s Normal stress associated with warping torsion (psi)

τ Unit shearing stress (psi)

τ_b Shearing stress due to plane bending (psi)

τ_p Shearing stress associated with St. Venant's primary torsion (psi)

τ_s Shearing stress associated with secondary warping (psi)

ϕ Total angle of twist (radians)

EI_x, EI_y Bending rigidity of a section (lb.-in.^{2})

GK Torsional rigidity of a section (lb.-in.^{2})

EC_w Warping rigidity of a section (lb.-in.^{4})

REFERENCES

1. Torsional Analysis of Rolled Steel Sections. *Bethlehem Steel Corp., 1963.*
2. *Bornscheuer, F.* Systematische Darstellung des Biege-und Verdrehvorganges unter besonderer Berücksichtigung der Wolbkräfttorsion, *Der Stahlbau 21, 1952, s. 1.*
3. *Bornscheuer, F.* Beispiel und Formelsammlung zur Spannungsberechnung dünnwandiger Stabe mit wolbbenhindertem Querschnitt, *Der Stahlbau 22, 1953, s. 32.*
4. *Bornscheuer, F.* Schweissanschlusse Torsionsbeanspruchter Trager mit I, [-und Z Querschnitten, *Schweissen und Schneiden, Jahrgang 13, Heft 3, Marz 1961.*
5. *Eggenschwyler, A.* Über die Festigkeitsberechnung von Schiebetoren und ähnlichen Bauwerken, *Diss. ETH 1921.*
6. *El Darwish, I. A. and Johnston, B. G.* Torsion of Structural Shapes, *Proc. ASCE, 203–227, Feb. 1965.*
7. *Goodier, J. N. and Barton, M. V.* The Effects of Web Deformation on the Torsion of I-Beams, *J. Applied Mechanics, 11, March 1944.*
8. *Kollbrunner, C. F. and Basler, K.* Torsionskonstanten und Schubspannungen bei St.-Venantscher Torsion, *Schweizer Stahlbauverband, Zürich, Heft 23, Juli. 1962.*
9. *Kollbrunner, C. F. and Basler, K.* Torsionsmomente und Stabverdrehung bei St.-Venantscher Torsion, *Schweizer Stahlbauverband, Zürich, Heft 27, Okt. 1963.*
10. *Kollbrunner, C. F. and Basler, K.* Sektorielle Grössen und Spannungen bei offenen, dünnwandigen Querschnitten, *Schweizer Stahlbauverband, Zürich, Heft 28, Jan. 1964.*
11. *Kollbrunner, C. F. and Basler, K.* Statik der Wölbtorsion und der gemischten Torsion. *Schweizer Stahlbauverband, Zürich, Heft 31, Mai. 1965.*
12. *Kollbrunner, C. F. and Hajdin, N.*, Die St.-Venantsche Torsion. *Schweizer Stahlbauverband, Zürich, Heft 26, Sept. 1963.*

13. *Kollbrunner, C. F. and Hajdin, N.* Wölbkrafttorsion dünnwandiger Stäbe mit offenem Profil, *Schweizer Stahlbauverband, Zürich, Heft 29, Okt. 1964.*
14. *Kollbrunner, C. F. and Hajdin, N.* Wölbkrafttorsion dünnwandiger Stäbe mit offenem Profil Teil II, *Schweizer Stahlbauverband, Zürich, Heft 30, Marz. 1965.*
15. *Lyse, I. and Johnston, B. G.* Structural Beams in Torsion, *Trans. ASCE 101, 857–926, 1936.*
16. *Maillart, R.* Zur Frage der Biegung, *Schweiz, Bauzeitung, Bd. 77, 1921.*
17. *Thürlimann, B. and Basler, K.* Plate Girder Research, *National Engineering Conference Proceedings, AISC, 1959.*
18. *Von Bach, C.* Versuch über die tatsächliche Widerstandsfähigkeit von Balken mit [-formigen Zuerschmitt, *Z.d. V.d.I., 1909, 1910.*

ACKNOWLEDGMENTS

The author expresses his sincere appreciation to Prof. F. W. Bornscheuer of the University of Stuttgart for his gratuitous offer in 1961 to compute, electronically, the torsional constants of American rolled sections appearing in Table 4. Other credits to Prof. F. W. Bornscheuer for valuable contributions included in this paper include: Table 3, influence lines for beams with welded end connections and the solutions for the differential equations from which Table 1 was prepared.

Note: An extensive bibliography on the subject of torsion has been compiled by the author, and is available from AISC.

CHARTS

CHART I Properties of Welded Shapes free to warp*

	Doubly Symmetrical	Singly Symmetrical
	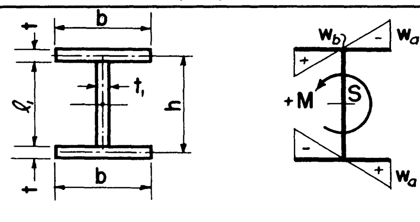	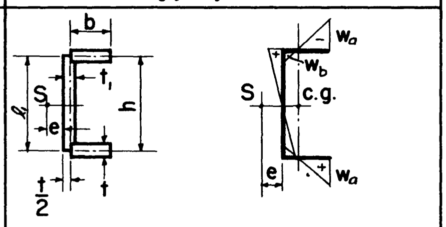
$w_a = w_{max}$ (in^2)	$\frac{bh}{4}$	$\frac{(A_1 + \frac{1}{3}A_2)\, b\ell_1}{4A_1 + \frac{2}{3}A_2}$
w_b (in^2)	—	$\frac{A_1\, b\ell_1}{4A_1 + \frac{2}{3}A_2}$
C_w (in^6)	$\frac{1}{24} b^3 h^2 t$	$\frac{1}{12} b^3 \ell_1^2 t \, \frac{3bt + 2\ell_1 t}{6bt + \ell_1 t_1}$
K (in^4)	$\frac{2}{3} bt^3 + \frac{1}{3} \ell_1 t_1^3$	$\frac{2}{3} bt^3 + \frac{1}{3} \ell_1 t_1^3$
e (in)	—	$\frac{3bA_1}{6A_1 + A_2}$

Where A_1 = flange area = bt, A_2 = web area = $\ell_1 t_1$, Total area = $2A_1 + A_2$

$$\lambda = \sqrt{\frac{GK}{EC_w}} = 0.62\sqrt{\frac{K}{C_w}} \text{ for steel}$$

* Exact values for rolled sections are given in Table 4.

CHART 2 Warping Properties of Welded Shapes

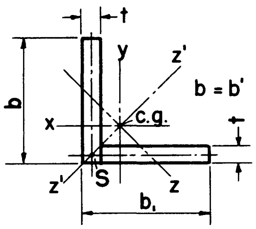

Singly Symmetrical

$$C_w = \frac{(2bt)^3}{144} \cong 0$$

Negligible warping

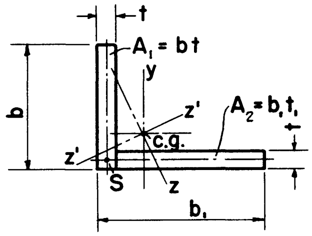

Nonsymmetrical

$$C_w = \frac{A_1^3 + A_2^3}{36} \cong 0$$

Negligible warping

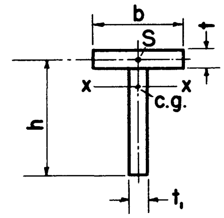

Singly Symmetrical

$C_w = 0$

Warpfree

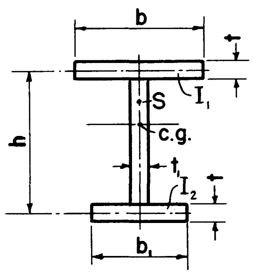

Singly Symmetrical

$C_w = h^2 I_1 I_2$

Free to warp

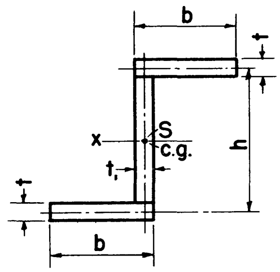

Antisymmetrical

$$C_w = \frac{h^2 I_y}{4}\left(\frac{1-3A}{2A}\right)$$ where A = total area

Free to warp

CHART 3

	x	M_p	M_s	$M_p + M_s$	$M_t = 0.5M$
$\lambda\ell = 2$ 24WF76	0.00	0.1760	0.3240	0.5000	0.50
	0.20	0.1497	0.3503	0.5000	0.50
	0.50	0	-0.5000 +0.5000	±0.5000	±0.50
	0.70	-0.1159	-0.3841	-0.5000	-0.50
	1.00	-0.1760	-0.3240	-0.5000	-0.50
$\lambda\ell = 3$ 18WF70	0.00	0.2875	0.2126	0.5000	0.50
	0.20	0.2480	0.2520	0.5000	0.50
	0.50	0	-0.5000 +0.5000	±0.5000	±0.50
	0.70	-0.1954	-0.3046	-0.5000	-0.50
	1.00	-0.2875	-0.2126	-0.5001	-0.50
$\lambda\ell = 5$ 8WF40	0.00	0.4185	0.0815	0.5000	0.50
	0.20	0.3742	0.1258	0.5000	0.50
	0.50	0	-0.5000 +0.5000	±0.5000	±0.50
	0.70	-0.3082	-0.1918	-0.5000	-0.50
	1.00	-0.4185	-0.0815	-0.5000	-0.50

	x	M_p	M_s	$M_p + M_s$	M_t
$\lambda\ell = 2$ 24WF76	0.00	0.1749	0.5251	0.7000	0.70
	0.20	0.1324	0.5676	0.7000	0.70
	0.30	0.0776	-0.3776 +0.6224	-0.3000 +0.7000	0.70
	0.80	-0.1102	-0.1898	-0.3000	-0.30
	1.00	-0.1245	-0.1755	-0.3000	-0.30
$\lambda\ell = 3$ 18WF70	0.00	0.2985	0.4015	0.7000	0.70
	0.20	0.2241	0.4759	0.7000	0.70
	0.30	0.1247	-0.4247 +0.5753	-0.3000 +0.7000	0.70
	0.80	-0.1785	-0.1215	-0.3000	-0.30
	1.00	-0.1975	-0.1025	-0.3000	-0.30
$\lambda\ell = 5$ 8WF40	0.00	0.4771	0.2229	0.7000	0.70
	0.20	0.3560	0.3440	0.7000	0.70
	0.30	0.1756	-0.4756 +0.5244	-0.3000 +0.7000	0.70
	0.80	-0.2557	-0.0443	-0.3000	-0.30
	1.00	-0.2713	-0.0287	-0.3000	-0.30

TABLE 1

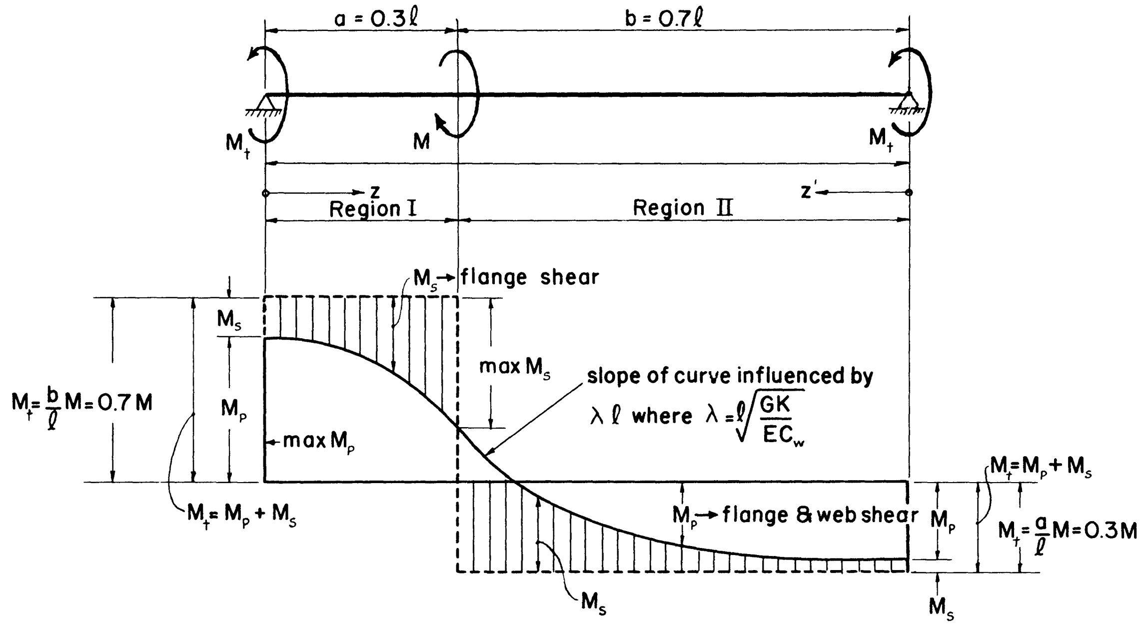

Flange web shear τ_P, τ_S are determined from M_P and M_S respectively. Web shear is determined from M_P only. These torsional shears must be combined with the shears resulting from plane bending.

M_t is determined, as above, from the symmetry of loading.

M_P max., shown above, is determined from the following Tables.

$M_S = M_t - M_P$

Shears:

Primary torsional shear stress, $\tau_p = G t \phi' = \dfrac{M_P t}{K}$

where t is the thickness of the flange or web

Secondary torsional shear stress, $\tau_S = \dfrac{w_{max} b}{4} \dfrac{M_S}{C_w}$

where b is the width of flange

TABLE 1 (continued)

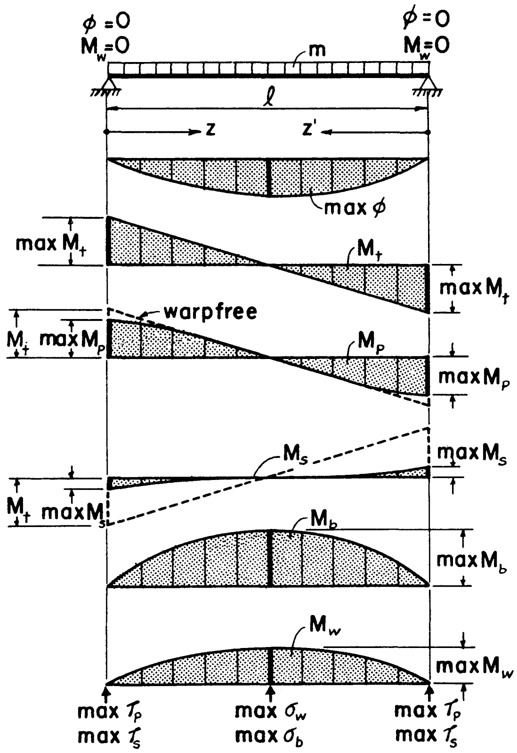

CASE 1

$$\max M_t = \frac{m\ell}{2}$$

$$\max M_p = \frac{m}{\lambda}\left[\frac{\lambda\ell}{2} - \tanh\frac{\lambda\ell}{2}\right], \text{ yields } \max \tau_p$$

$$\max M_s = \max M_t - \max M_p \text{ , yields } \max \tau_s$$

$$\max M_w = \frac{m}{\lambda^2}\left[1 - \frac{1}{\cosh\lambda\frac{\ell}{2}}\right], \text{ yields } \max \sigma_w$$

M_w for any value of z:

$$M_w = \frac{m}{\lambda^2}\left[1 - \frac{\sinh\lambda z + \sinh\lambda z'}{\sinh\lambda\ell}\right]$$

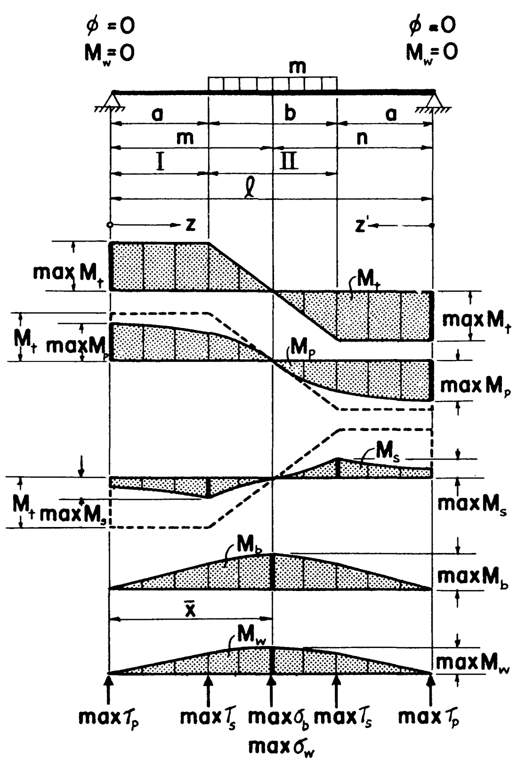

CASE 2

$$\max M_t = \frac{mb}{2\ell}\left[2a + b\right]$$

$$\max M_p = \frac{m}{\lambda}\left[\frac{\lambda b}{2} - \frac{\cosh\lambda(a+b) - \cosh\lambda a}{\sinh\lambda\ell}\right], \text{ yields } \max \tau_p$$

$M_s = \max M_t - \max M_p$, yields max combination of shear stresses

$$\max M_w = \frac{m}{\lambda^2}\left[1 - \frac{\cosh\lambda a}{\cosh\lambda\frac{\ell}{2}}\right], \text{ yields } \max \sigma_w$$

M_w for any value of z:

$$\text{Region II, } M_w = \frac{m}{\lambda^2}\left[1 - \frac{\cosh\lambda a \cdot \sinh\lambda z' + \cosh\lambda a \cdot \sinh\lambda z}{\sinh\lambda\ell}\right]$$

$$\text{Region I, } M_w = \frac{m}{\lambda^2}\left[\frac{\cosh\lambda(a+b) - \cosh\lambda a}{\sinh\lambda\ell}\right]\sinh\lambda z$$

For max M_w, occurring in Region II, let $z = \bar{x} = a + \frac{M_t}{m}$

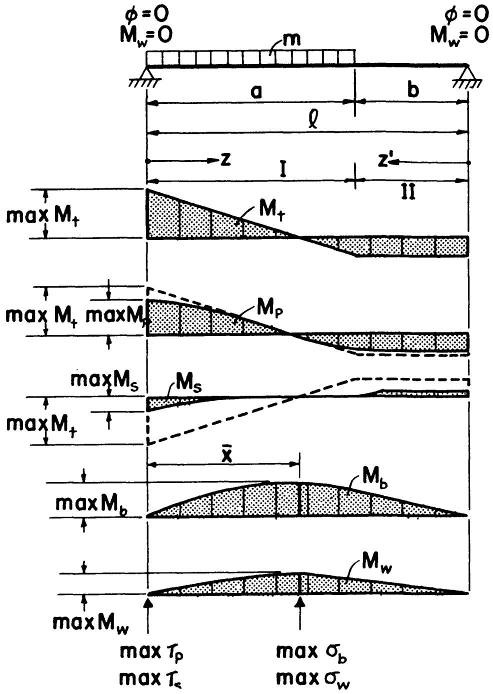

CASE 3

$$\max M_t = \frac{m\,a}{2\ell}(2\ell - a)$$

$$\max M_p = \frac{m}{\lambda}\left[\lambda\left(a - \frac{a^2}{2\ell}\right) - \frac{\cosh\lambda\ell - \cosh\lambda b}{\sinh\lambda\ell}\right]$$, yields max τ_p

$\max M_s = \max M_t - \max M_p$, yields max τ_s

$\max M_w = A m \ell^2$

$\lambda\ell$	A								
	a=.10 $\bar{x}$=.09	a=.20 $\bar{x}$=.16	a=.30 $\bar{x}$=.23	a=.40 $\bar{x}$=.29	a=.50 $\bar{x}$=.34	a=.60 $\bar{x}$=.38	a=.70 $\bar{x}$=.43	a=.80 $\bar{x}$=.47	a=.90 $\bar{x}$=.49
1.0	.004	.015	.030	.047	.065	.080	.094	.105	.111
2.0	.004	.014	.026	.039	.052	.064	.074	.082	.086
3.0	.004	.012	.022	.031	.040	.048	.055	.060	.063
4.0	.003	.010	.018	.025	.032	.036	.040	.043	.045
5.0	.003	.009	.015	.020	.024	.027	.030	.032	.033

M_w for any value of z:

$$M_w = \frac{m}{\lambda^2}\left(1 - \frac{\sinh\lambda z' + \cosh\lambda b\,\sinh\lambda z}{\sinh\lambda\ell}\right)$$ Region I

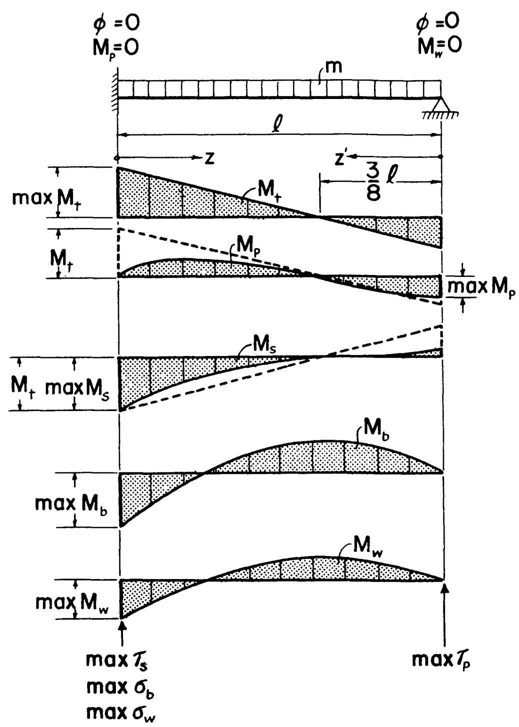

CASE 4

$\max M_t = \max M_s$

$$\max M_p = \frac{m}{\lambda}\left[\frac{2k - (\lambda\ell)^2}{2\lambda\ell} + \frac{\cosh\lambda\ell - (1+k)}{\sinh\lambda\ell}\right]$$, yields max τ_p

$$M_s = \frac{m}{\lambda}\left[-\frac{\cosh\lambda\ell - (1+k)}{\sinh\lambda\ell}\right]$$, yields max τ_s

$\max M_w = -\frac{mk}{\lambda^2}$, yields max σ_w

M_w for any value of z:

$$M_w = \frac{m}{\lambda^2}\left[1 - \frac{\sinh\lambda z + (1+k)\sinh\lambda z'}{\sinh\lambda\ell}\right]$$

where $$k = \lambda\ell\,\frac{\left(\lambda\frac{\ell}{2} - \tanh\lambda\frac{\ell}{2}\right)\tanh\lambda\ell}{\lambda\ell - \tanh\lambda\ell}$$

TABLE 1 (continued)

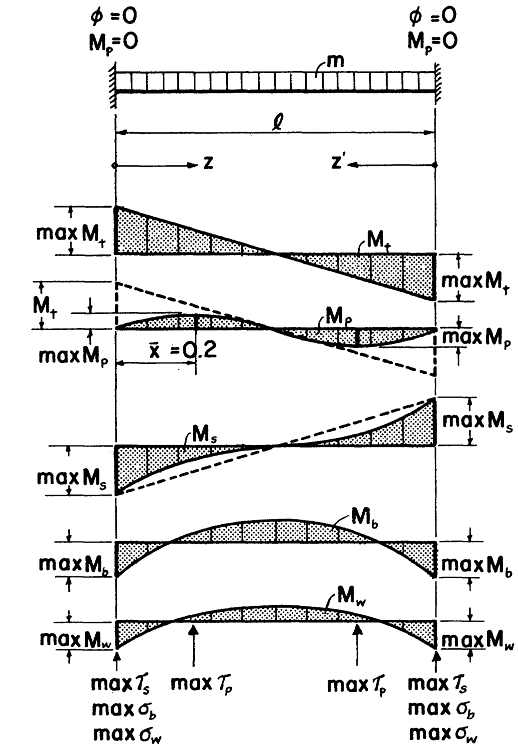

CASE 5

max $M_t = \frac{m\ell}{2}$

max $M_p = m\ell\left[0.30 + \frac{\cosh 0.2\lambda\ell - \cosh 0.8\lambda\ell}{4\sinh^2\frac{\lambda\ell}{2}}\right]$, yields max τ_p

max M_s = max M_t, yields max τ_s

max $M_w = \frac{m}{\lambda^2}\left[1 - \frac{\lambda\frac{\ell}{2}}{\tanh\lambda\frac{\ell}{2}}\right]$, yields max σ_w

M_w for any value of z :

$$M_w = \frac{m}{\lambda^2}\left[1-(1-k)\frac{\sinh\lambda z + \sinh\lambda z'}{\sinh\lambda\ell}\right] \text{ where } k = 1-\frac{\lambda\frac{\ell}{2}}{\tanh\lambda\frac{\ell}{2}}$$

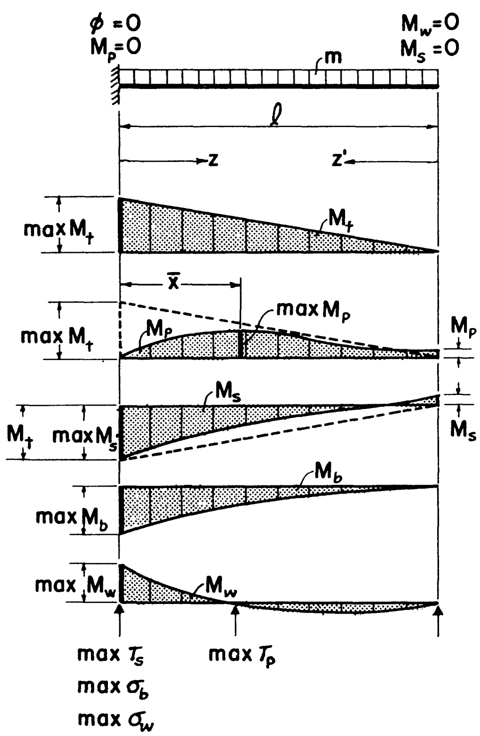

CASE 6

max $M_t = m\ell$

max M_p : max $M_p = Dm\ell$

$\lambda\ell$	0.5	1.0	1.5	2.0	3.0	4.0	5.0
$\bar{x}$	1.0000	0.7719	0.6344	0.5371	0.4256	0.3667	0.3290
D	.0374	.1145	.1872	.2466	.3420	.4200	.4845

max M_s = max M_t − max M_p , yields max τ_s

max $M_w = \frac{m}{\lambda^2}\left[\frac{1-(1+\lambda\ell\sinh\lambda\ell)}{\cosh\lambda\ell}\right]$, yields max σ_w

M_w for any value of z :

$$M_w = \frac{m}{\lambda^2}\left[1+\lambda\ell\sinh\lambda z - \frac{(1+\lambda\ell\sinh\lambda\ell)\cosh\lambda z}{\cosh\lambda\ell}\right]$$

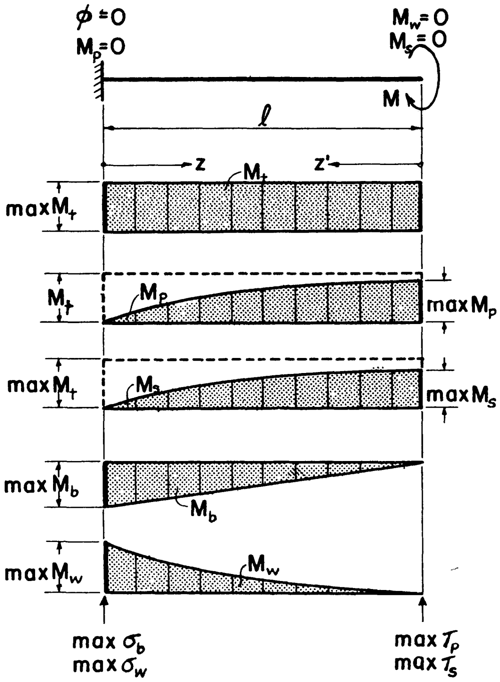

CASE 7

$\max M_t = M$

$\max M_p = M\left[1 - \dfrac{1}{\cosh\lambda\ell}\right]$, yields $\max \tau_p$

$\max M_s = \max M_t - \max M_p$, yields $\max \tau_s$

$\max M_w = -\dfrac{M}{\lambda}\left(\tanh\lambda\ell\right)$, yields $\max \sigma_w$

M_w for any value of z:

$$M_w = \frac{M}{\lambda}\left[-\frac{\sinh\lambda z'}{\cosh\lambda\ell}\right]$$

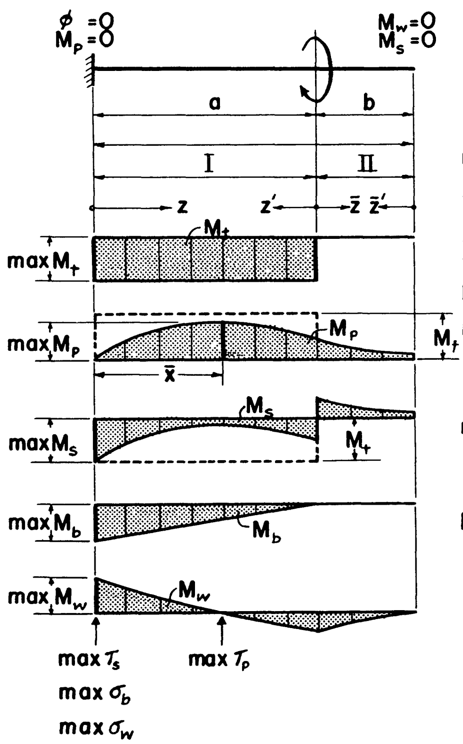

CASE 8

$\max M_t = M$

$\max M_p$: $M_p = DM$, $\bar{x} = a/\ell$

	a = 0.8					a = 0.6					a = 0.4					a = 0.2				
$\lambda\ell$	1	2	3	4	5	1	2	3	4	5	1	2	3	4	5	1	2	3	4	5
$\bar{x}$	.75	.64	.56	.51	.48	.55	.46	.43	.43	.40	.36	.32	.29	.29	.27	.19	.17	.16	.16	.15
D	.22	.48	.64	.74	.82	.12	.31	.46	.58	.69	.06	.17	.29	.40	.50	.02	.06	.11	.17	.23

$\max M_s = \max M_t$, yields $\max \tau_s$

$\max M_w = \dfrac{M}{\lambda}\left[-\sinh\lambda a + \tanh\lambda\ell\left(\cosh\lambda a - 1\right)\right]$, yields $\max \sigma_w$

M_w for any value of z:

Region I, $M_w = \dfrac{M}{\lambda}\,\dfrac{-\cosh\lambda\ell\,\sinh\lambda z' + \left(\cosh\lambda a - 1\right)\sinh\lambda\bar{z}'}{\cosh\lambda\ell}$

Region II, $M_w = \dfrac{\left(\cosh\lambda a - 1\right)\sinh\lambda\bar{z}'}{\cosh\lambda\ell}\,\dfrac{M}{\lambda}$

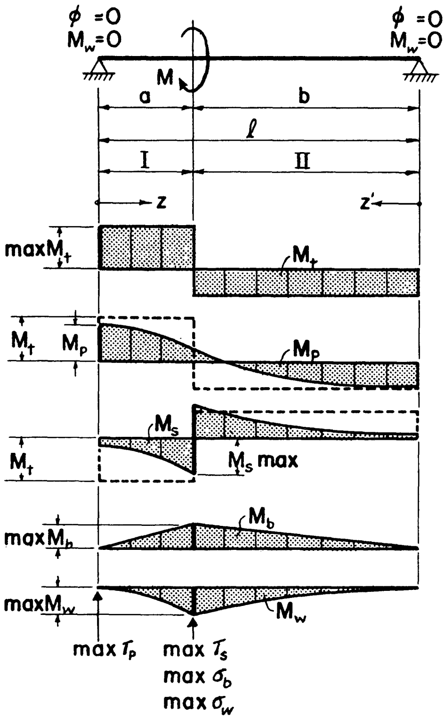

CASE 9 For Quick Method see Table 3

$$\max M_t = \frac{Mb}{\ell}$$

$$\max M_p = M\left[\frac{b}{\ell} - \frac{\sinh \lambda b}{\sinh \lambda \ell}\right] \text{, yields } \max \tau_p$$

$$\max M_s = \max M_t - M_p \text{, yields } \max \tau_s$$

$$\max M_w = \frac{M}{\lambda}\,\frac{\sinh \lambda b}{\sinh \lambda \ell}\,\sinh \lambda a \text{, yields } \max \sigma_w$$

M_w for any value of z :

Region I, $M_w = \dfrac{M}{\lambda}\,\dfrac{\sinh \lambda b}{\sinh \lambda \ell}\,\sinh \lambda z$

Region II, $M_w = \dfrac{M}{\lambda}\,\dfrac{\sinh \lambda a}{\sinh \lambda \ell}\,\sinh \lambda z'$

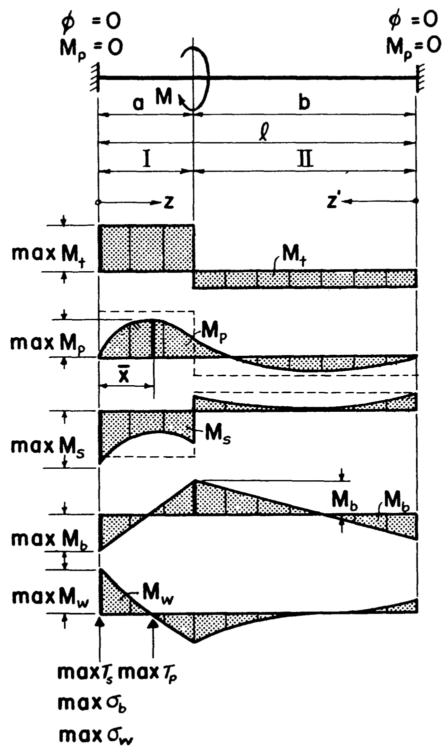

CASE 10 (when a < b), See Table 3 for Short Method.

$M_t = M_p + M_s$

$$\max M_p = AM, \quad M_p = M\left[\frac{\lambda b + k_2 - k_1}{\lambda \ell} - \frac{(\sinh\lambda b + k_2)\cosh\lambda z - k_1\cosh\lambda z'}{\sinh\lambda\ell}\right]$$

max M_p

	A		
$\lambda\ell$	$a = 0.50\ell$, $\bar{x} \cong 0.25$	$a = 0.30\ell$, $\bar{x} \cong 0.18$	$a = 0.10\ell$, $\bar{x} \cong 0.10$
1.0	0.015	0.014	0.003
2.0	0.057	0.051	0.012
3.0	0.114	0.105	0.026
4.0	0.176	0.167	0.040
5.0	0.235	0.229	0.064

$$\max M_s = M\,\frac{(\sinh\lambda b + k_2) - k_1\cosh\lambda\ell}{\sinh\lambda\ell}$$

$$\max M_w = \frac{M}{\lambda}\,k_1$$

M_w for any value of z :

Region I, $M_w = \dfrac{M}{\lambda}\,\dfrac{(\sinh\lambda b + k_2)\sinh\lambda z + k_1\sinh\lambda z'}{\sinh\lambda\ell}$

Region II, $M_w = \dfrac{M}{\lambda}\,\dfrac{k_2\sinh\lambda z + (\sinh\lambda a + k_1)\sinh\lambda z'}{\sinh\lambda\ell}$

$$k_{1,2} = \frac{\dfrac{\sinh\lambda a + \sinh\lambda b}{\sinh\lambda\ell} - 1}{2\tanh\lambda\frac{\ell}{2}} \pm \frac{\left(\dfrac{a-b}{\ell} - \dfrac{\sinh\lambda a - \sinh\lambda b}{\sinh\lambda\ell}\right)\dfrac{\ell}{2}\tanh\lambda\dfrac{\ell}{2}}{\ell - \dfrac{2}{\lambda}\tanh\lambda\dfrac{\ell}{2}}$$

TABLE 1 (continued)

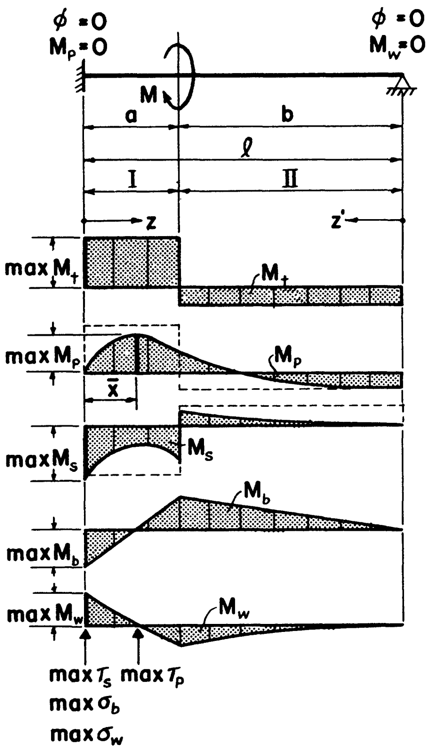

CASE II

Region I $\quad M_p = M \left[\dfrac{\lambda b - k}{\lambda \ell} - \dfrac{\sinh\lambda b \, \cosh\lambda z - k \cosh\lambda z'}{\sinh\lambda \ell} \right]$

Region II $\quad M_p = M \left[-\dfrac{\lambda a + k}{\lambda \ell} + \dfrac{\sinh\lambda a + k}{\sinh\lambda \ell} \cosh\lambda z' \right]$

max M_p = A M , when $a \geqq b$ max M_p occurs at hinge support.
when $a < b$ max M_p occurs at fixed support.

$\lambda\ell$	Region I				Region II		
	$a = .10$ $\bar{x} = .08$	$a = .20$ $\bar{x} = .15$	$a = .30$ $\bar{x} = .19$	$a = .40$ $\bar{x} = .21$	$a = .50$ $\bar{x} = 1.0$	$a = .70$ $\bar{x} = 1.0$	$a = .90$ $\bar{x} = 1.0$
1.0		.0112	.0176	.0242	-.0296	-.0350	-.0195
2.0	.0140	.0397	.0638	.0790	-.1025	-.1230	-.0702
3.0	.0296	.0809	.1258	.1525	-.1875	-.2299	-.1365
4.0	.0492	.1274	.1922	.2273	-.2602	-.3373	-.2058
5.0	.0717	.1781	.2573	.2945	-.3209	-.4138	-.2718

A

max $M_s = \dfrac{\sinh\lambda b - k \cosh\lambda \ell}{\sinh\lambda \ell}$, when $a \leqq b$, occurs at fixed support.

max $M_s = \dfrac{\sinh\lambda b \, \cosh\lambda a - k \cosh\lambda b}{\sinh\lambda \ell}$, when $a > b$, occurs at load M.

max $M_w = \dfrac{M}{\lambda} k$

M_w for any value of z :

Region I, $\quad M_w = \dfrac{M}{\lambda} \, \dfrac{\sinh\lambda b \cdot \sinh\lambda z + k \sinh\lambda z'}{\sinh\lambda \ell}$

Region II, $\quad M_w = \dfrac{M}{\lambda} \, \dfrac{\sinh\lambda a + k}{\sinh\lambda \ell} \sinh\lambda z'$

$$k = \frac{\lambda b \sinh\lambda \ell - \lambda \ell \sinh\lambda b}{\sinh\lambda \ell - \lambda \ell \cosh\lambda \ell}$$

TABLE 2—SHORT METHOD

TYPE 2 CONSTRUCTION

Values for max M_p and max M_w, uniform torsional moment m

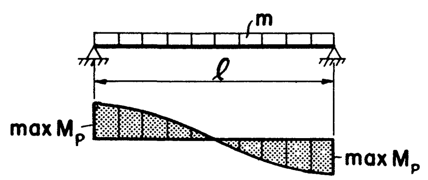

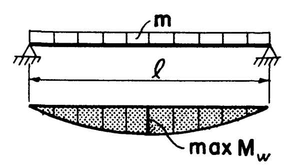

max $M_p = D_1 m \ell$

max $M_w = D_2 m \ell^2$

$\lambda\ell$	0.5	1.0	1.5	2.0	2.5	3	4	5	6
D_1	0.0102	0.0379	0.0765	0.1192	0.1607	0.1983	0.2590	0.3027	0.3342
D_2	0.1220	0.1132	0.1011	0.0880	0.0753	0.0639	0.0459	0.0338	0.0252

Values for max M_w, concentrated torsional moment M

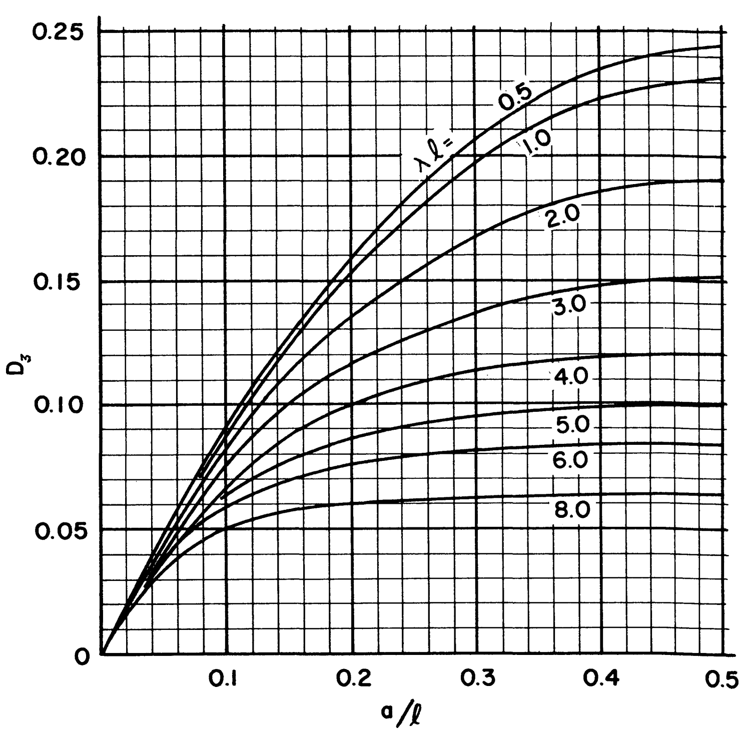

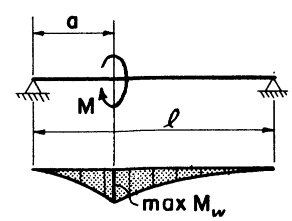

max $M_w = D_3 M \ell$

TABLE 3

INFLUENCE LINES FOR $M_{w/z=o}\ f(\lambda\ell)$, SHORT METHOD

$$M_{w/z=o} = \underbrace{\frac{1}{\lambda}\Sigma\eta M}_{} + \underbrace{\frac{1}{\lambda^2}Am}_{}$$

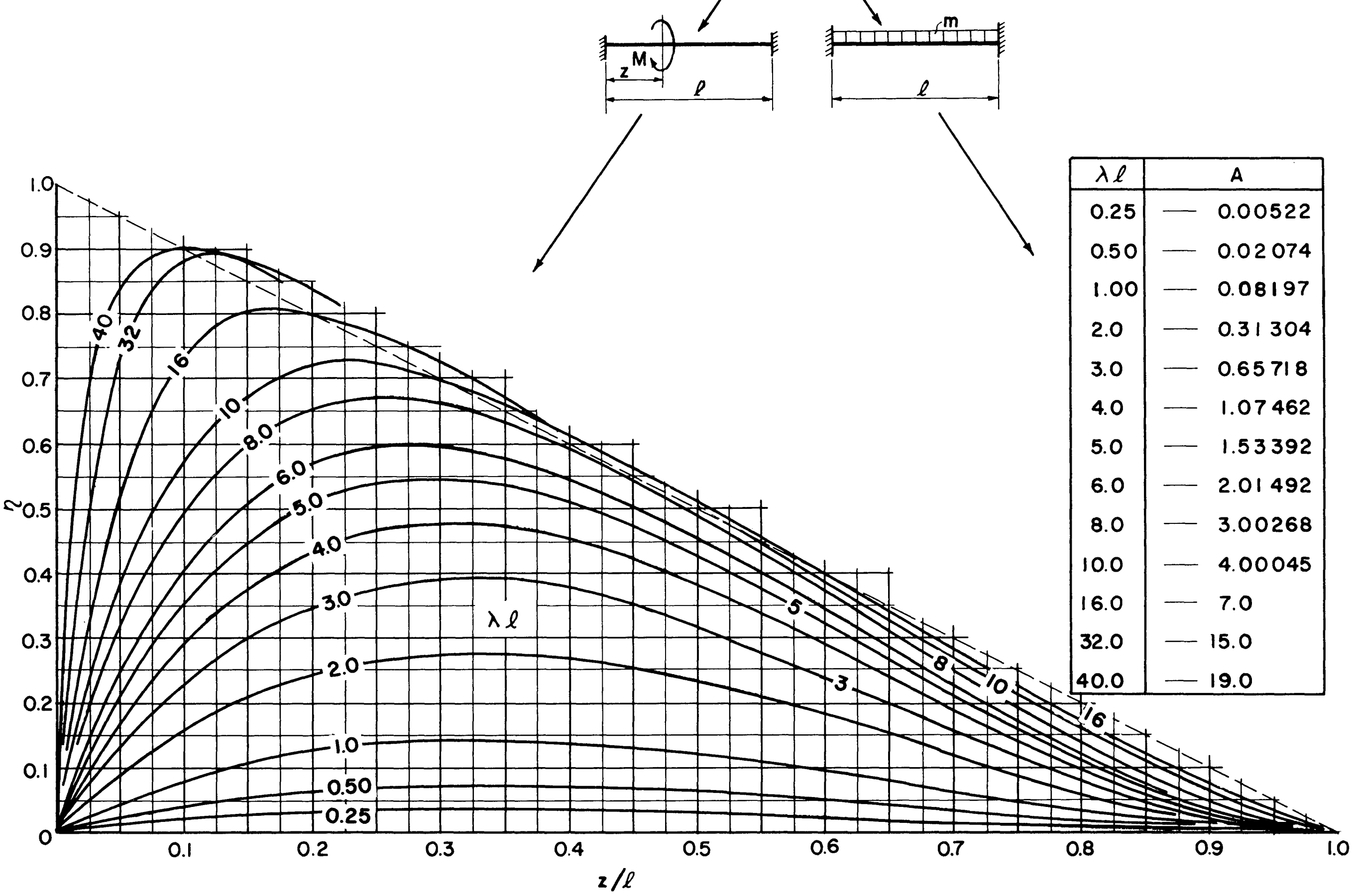

$\lambda\ell$	A
0.25	— 0.00522
0.50	— 0.02074
1.00	— 0.08197
2.0	— 0.31304
3.0	— 0.65718
4.0	— 1.07462
5.0	— 1.53392
6.0	— 2.01492
8.0	— 3.00268
10.0	— 4.00045
16.0	— 7.0
32.0	— 15.0
40.0	— 19.0

TABLE 4

Structural Section	w_{max} in.^{2}	C_w in.^{6}	S_w in.^{4}	λ in.$^{-1}$
36 WF 300	145.9	372,500	2,553	0.008284
280	144.9	340,700	2,351	0.007843
260	144.0	306,000	2,125	0.007387
245	143.3	281,800	1,967	0.007034
230	142.6	258,400	1,812	0.006695
194	106.7	108,900	1,021	0.009050
182	106.1	99,980	942.8	0.008594
170	105.4	91,310	866.2	0.008133
160	104.9	83,250	793.4	0.007756
150	104.5	75,340	721.3	0.007379
135	103.8	61,710	594.6	0.006877
33 WF 240	127.3	223,000	1,752	0.008106
220	126.4	198,000	1,567	0.007567
200	125.4	173,700	1,385	0.007011
152	93.81	66,670	710.8	0.008613
141	93.29	59,420	637.0	0.008112
130	92.78	51,730	557.5	0.007623
118	92.22	43,380	470.4	0.007144
30 WF 210	109.8	148,100	1,349	0.008788
190	108.8	129,500	1,190	0.008114
172	107.9	113,100	1,048	0.007502
132	77.29	39,240	507.8	0.009972
124	76.88	35,830	466.0	0.009480
116	76.52	32,150	420.1	0.009010
108	76.17	28,160	369.7	0.008570
99	75.74	24,180	319.3	0.008104
27 WF 177	92.01	87,620	952.4	0.009600
160	91.17	76,720	841.5	0.008858
145	90.44	67,600	747.5	0.008204
114	66.33	25,670	387.0	0.010720
102	65.73	22,050	335.5	0.009809
94	65.34	19,470	297.9	0.009199
84	64.89	16,050	247.3	0.008495
24 WF 160	83.08	67,890	817.1	0.009813
145	82.40	59,250	719.1	0.009057
130	81.73	50,650	619.8	0.008293
120	70.65	34,370	486.5	0.009792
110	70.16	30,810	439.2	0.009140
100	69.68	27,190	390.2	0.008474
94	53.05	13,860	261.3	0.01227
84	52.55	11,880	226.0	0.01121
76	52.18	10,210	195.6	0.01034
68	51.81	8,436	162.8	0.009525
21 WF 142	66.86	39,640	592.9	0.01180
127	66.14	34,410	520.2	0.01081
112	65.44	29,090	444.5	0.009771
96	45.65	11,030	241.7	0.01541
82	44.96	8,923	198.5	0.01364
73	42.51	6,878	161.8	0.01330
68	42.27	6,239	147.6	0.01259
62	41.97	5,453	129.9	0.01170
55	41.65	4,471	107.3	0.01074
18 WF 114	51.74	19,360	374.3	0.01376
105	51.32	17,340	337.8	0.01289
96	50.90	15,380	302.1	0.01201
85	38.47	7,460	193.9	0.01718
77	38.07	6,588	173.1	0.01592
70	37.73	5,783	153.3	0.01475
64	37.44	5,143	137.4	0.01375
18 WF 60	33.17	3,591	108.3	0.01556
55	32.93	3,175	96.40	0.01451
50	32.68	2,794	85.48	0.01343
45	32.45	2,374	73.16	0.01237
16 WF 96	44.53	12,240	274.9	0.01425
88	44.18	10,820	245.0	0.01332
78	33.15	5,167	155.9	0.01936
71	32.82	4,548	138.6	0.01800
64	32.48	3,957	121.8	0.01662
16 WF 58	32.19	3,463	107.6	0.01542
50	27.62	2,101	76.04	0.01700
45	27.38	1,825	66.68	0.01563
40	27.12	1,576	58.12	0.01423
36	26.96	1,302	48.29	0.01318
14 WF 426	65.35	144,200	2,206	0.03001
398	64.15	129,400	2,017	0.02875
370	62.94	115,700	1,838	0.02745
342	61.75	102,700	1,663	0.02606
314	60.50	90,460	1,495	0.02459
287	59.35	79,270	1,336	0.02308
264	58.34	70,470	1,208	0.02175
246	57.55	63,830	1,109	0.02065
237	57.16	60,590	1,060	0.02008
228	56.77	57,530	1,013	0.01951
219	56.36	54,400	965.1	0.01891
211	56.04	51,700	922.6	0.01838
202	55.63	48,830	877.9	0.01777
193	55.23	45,940	831.8	0.01714
184	54.82	43,230	788.6	0.01652
176	54.49	40,650	746.0	0.01593
167	54.10	37,990	702.2	0.01527
158	53.69	35,510	661.3	0.01461
150	53.34	33,200	622.3	0.01399
142	53.04	30,900	582.6	0.01338
320	61.48	88,130	1,433	0.02497
136	50.44	26,570	526.9	0.01403
127	50.03	24,460	489.0	0.01326
119	49.67	22,600	455.0	0.01256
111	49.33	20,710	419.8	0.01183
103	48.96	18,940	386.8	0.01109
95	48.62	17,150	352.7	0.01035
87	48.26	15,490	320.9	0.009584
84	40.28	10,120	251.2	0.01297
78	40.03	9,202	229.9	0.01216
74	33.76	5,992	177.5	0.01576
68	33.49	5,390	160.9	0.01467
14 WF 61	33.17	4,716	142.2	0.01337
53	26.77	2,534	94.67	0.01710
48	26.54	2,236	84.25	0.01572
43	26.30	1,948	74.07	0.01434
38	23.05	1,231	53.42	0.01592
34	22.86	1,065	46.60	0.01447
30	22.69	884.7	39.00	0.01304
12 WF 190	40.05	23,520	587.3	0.02851
161	38.78	18,640	580.8	0.02530
133	37.54	14,360	382.5	0.02187
120	37.00	12,440	336.1	0.02014
106	36.37	10,630	292.4	0.01825
99	36.05	9,727	269.8	0.01724
92	35.75	8,864	248.0	0.01624

TABLE 4 (continued)

Structural Section		w_{max} in.^{2}	C_w in.^{6}	S_w in.^{4}	λ in.$^{-1}$
12 WF	85	35.42	8,059	227.5	0.01520
	79	35.16	7,329	208.4	0.01429
	72	34.85	6,542	187.7	0.01321
	65	34.54	5,784	167.5	0.01211
	58	28.91	3,577	123.7	0.01502
	53	28.71	3,165	110.2	0.01389
	50	23.32	1,877	80.49	0.01915
	45	23.09	1,646	71.30	0.01755
	40	22.85	1,437	62.88	0.01593
	36	19.20	805.2	41.94	0.02027
	31	18.96	663.6	34.99	0.01798
	27	18.79	549.5	29.25	0.01615
10 WF	112	26.38	6,031	228.6	0.03116
	100	25.87	5,159	199.5	0.02863
	89	25.38	4,405	173.5	0.02616
	77	24.86	3,645	146.6	0.02334
	72	24.64	3,327	135.0	0.02208
	66	24.36	2,994	122.9	0.02058
	60	24.10	2,664	110.5	0.01904
	54	23.82	2,345	98.42	0.01742
	49	23.61	2,073	87.81	0.01602
	45	19.06	1,200	62.98	0.02192
10 WF	39	18.80	994.0	52.88	0.01942
	33	18.55	791.0	42.65	0.01691
	29	14.09	356.0	25.26	0.02550
	25	13.90	292.4	21.04	0.02263
	21	13.74	220.1	16.02	0.01987
8 WF	67	16.71	1,440	86.15	0.03699
	58	16.32	1,180	72.30	0.03311
	48	15.86	929.9	58.63	0.02857
	40	15.53	724.8	56.67	0.02453
	35	15.30	618.0	40.38	0.02198
	31	15.13	528.9	34.95	0.01984
	28	12.42	311.4	25.07	0.02575
	24	12.24	258.3	21.11	0.02266
	20	10.22	126.6	12.39	0.02813
	17	10.10	98.1	9.724	0.02515
16 B	31	21.27	713.4	33.54	0.01610
	26	21.04	537.9	25.56	0.01412
14 B	26	16.92	389.0	22.99	0.01905
	22	16.73	300.9	17.99	0.01680
12 B	22	11.98	159.4	13.32	0.02676
	19	11.84	127.0	10.73	0.02390
	16.5	11.73	95.0	8.102	0.02196
10 B	19	9.905	100.9	10.19	0.03003
	17	9.815	82.1	8.370	0.02748
	15	9.731	65.4	6.721	0.02556

Structural Section		w_{max} in.^{2}	C_w in.^{6}	S_w in.^{4}	λ in.$^{-1}$
8 B	15	7.835	49.9	6.375	0.03321
	13	7.746	39.0	5.040	0.03059
6 B	16	5.890	36.7	6.234	0.04882
	12	5.721	23.4	4.104	0.03948
6 WF	25	8.989	149.3	16.62	0.03485
	20	8.776	113.3	12.92	0.02893
	15.5	8.597	79.5	9.250	0.02390
5 WF	18.5	5.904	49.0	8.307	0.04840
	16	5.800	40.3	6.960	0.04315
12 B	14	11.60	76.2	6.571	0.01960
10 B	11.5	9.545	46.5	4.879	0.02107
8 B	10	7.581	29.3	3.866	0.02463
6 B	8.5	5.551	14.9	2.685	0.03058
5 M	18.9	5.729	45.6	7.963	0.05229
4 M	13	3.571	12.4	3.487	0.07372
24 **I**	120	46.07	10,640	231.0	0.02136
	105.9	45.08	10,010	222.0	0.01939
	100	41.90	6,108	145.8	0.02200
	90	41.19	5,823	141.4	0.01974
	79.9	40.45	5,544	137.0	0.01789
20 **I**	95	34.35	4,339	126.3	0.02778
	85	33.65	4,094	121.7	0.02480
	75	30.69	2,633	85.77	0.02602
	65.4	30.02	2,473	82.39	0.02289
18 **I**	70	27.05	1,710	63.21	0.03146
	54.7	25.96	1,526	58.78	0.02398
15 **I**	50	20.27	779.5	38.45	0.03274
	42.9	19.77	727.1	36.78	0.02797
12 **I**	50	15.53	479.7	30.89	0.04967
	40.8	14.89	426.2	28.63	0.03948
	35	14.54	313.7	21.57	0.03628
	31.8	14.32	300.6	20.99	0.03312
10 **I**	35	11.75	176.6	15.03	0.05596
	25.4	11.08	150.1	13.56	0.03813
8 **I**	23	7.899	58.6	7.426	0.06228
	18.4	7.575	52.2	6.901	0.04831
7 **I**	20	6.377	32.6	5.113	0.07715
	15.3	6.046	28.1	4.658	0.05585
6 **I**	17.25	5.028	17.1	3.402	0.09957
	12.5	4.696	14.1	3.019	0.06591
5 **I**	14.75	3.837	8.3	2.164	0.1379
	10.0	3.506	6.4	1.847	0.08025
4 **I**	9.5	2.591	2.9	1.134	0.1346
	7.7	2.465	2.5	1.039	0.1027
3 **I**	7.5	1.719	1.0	0.5971	0.2093
	5.7	1.596	0.8	0.5242	0.1410

TABLE 4 (continued)

Structural Section	e in.	w_b in.^{2}	w_a in.^{2}	C_w in.^{6}	S_w in.^{4}	λ in.$^{-1}$
18 [58.0	0.6617	8.753	−24.48	1,012	41.34	0.03307
51.9	0.7618	9.186	−23.62	931.2	39.42	0.02904
45.8	0.8707	9.697	−22.68	847.8	37.39	0.02555
42.7	0.9293	9.988	−22.17	804.8	36.30	0.02406
15 [50.0	0.4739	5.840	−17.50	391.5	22.37	0.04968
40.0	0.6418	6.339	−16.33	327.8	20.08	0.03935
33.9	0.7581	6.739	−15.51	287.8	18.55	0.03476
12 [30.0	0.4982	4.231	−11.96	116.6	9.752	0.05125
25.0	0.6120	4.529	−11.32	101.3	8.942	0.04270
20.7	0.7239	4.862	−10.69	87.35	8.169	0.03764
10 [30.0	0.2762	2.853	−9.564	60.49	6.325	0.08815
25.0	0.3897	3.043	−9.042	52.12	5.765	0.06956
20.0	0.5167	3.297	−8.454	43.69	5.169	0.05413
15.3	0.6575	3.634	−7.796	35.40	4.542	0.04468
9 [20.0	0.4122	2.661	−7.350	30.16	4.104	0.07154
15.0	0.5604	2.945	−6.732	23.99	3.564	0.05434
13.4	0.6183	3.074	−6.489	21.82	3.364	0.05081
8 [18.75	0.3406	2.161	−6.176	19.16	3.103	0.09204
13.75	0.4974	2.406	−5.600	14.85	2.652	0.06588
11.5	0.5785	2.555	−5.300	12.84	2.423	0.05873
7 [14.75	0.3523	1.810	−4.823	10.03	2.081	0.09926
12.25	0.4392	1.923	−4.546	8.58	1.888	0.08118
9.8	0.5370	2.074	−4.231	7.11	1.682	0.06923
6 [13.0	0.3001	1.421	−3.805	5.48	1.442	0.1296
10.5	0.3954	1.516	−3.548	4.54	1.282	0.1012
8.2	0.4984	1.645	−3.267	3.67	1.123	0.08400
5 [9.0	0.3492	1.157	−2.665	2.23	0.8378	0.1344
6.7	0.4613	1.261	−2.414	1.71	0.7111	0.1059
4 [7.25	0.3163	0.8480	−1.867	0.92	0.4978	0.1831
5.4	0.4194	0.9099	−1.688	0.69	0.4137	0.1409
3 [6.0	0.2445	0.5480	−1.241	0.33	0.2731	0.2991
5.0	0.3274	0.5938	−1.135	0.28	0.2472	0.2406
4.1	0.3931	0.6238	−1.052	0.23	0.2188	0.2057